HYDROGEN PRODUCTION FROM BIOMASS

A Dissertation presented to

The Faculty of the Graduate School at
The University of Missouri-Columbia

In Partial Fulfillment
of the Requirements for the Degree

Doctor of Philosophy

---

by

JOHN J HAHN

Prof William A Jacoby, Dissertation Supervisor

DECEMBER 2006

The undersigned, appointed by the dean of the Graduate School, have examined the dissertation entitled

HYDROGEN PRODUCTION FROM BIOMASS

Presented by John J Hahn,

A candidate for the degree of Doctor of Philosophy,
and hereby certify that, in their opinion, it is worthy of acceptance.

_____
Professor William A Jacoby

_____
Professor Rakesh K Bajpai

_____
Professor Eric J Doskocil

_____
Professor Quingsong Yu

_____
Professor Ingolf U Gruen

DEDICATION

I would like to dedicate this dissertation to my family who has supported and encouraged me throughout this endeavor. To my wife Jessica: thank you for your loving support and everlasting patience to help me through this endeavor. To my parents: thank you for your love and support throughout my entire life and helping me realize who I am today.

ACKNOWLEDGEMENTS

I would like to acknowledge my advisor, Professor William Jacoby, who has been my advisor, mentor, and friend throughout my entire graduate education.

I am indebted to all the people whose knowledge and experience have been so valuable to the success of my work. I would like to thank Leemer Cernohlavek for all his help, especially with the fabrication of the SCW reactors. I would like to thank Maria Ghirardi of the National Renewable Energy Laboratories for all her assistance and expertise on the photosynthetic hydrogen work. I would like to thank H. Bryan Lanterman and Professor Sunggyu Lee for their knowledge of supercritical fluids and the use of their analytical equipment. I would also like to thank my committee members, Professor Rakesh Bajpai, Professor Eric Doskocil, Professor Quingsong Yu, and Professor Ingolf Gruen, for their guidance and support.

Finally, I would like to express my heartfelt gratitude to all my friends in the Chemical Engineering Department who have made my experience at Mizzou one that I will always treasure.

TABLE OF CONTENTS

LIST OF FIGURES

FIGURE PAGE

LIST OF TABLES

TABLE PAGE

1 INTRODUCTION

1.1 RENEWABLE ENERGY

According to the Department of Energy, total petroleum consumption is projected to grow from 20.8 million barrels per day in 2004 to 26.1 million barrels per day in 2025 [1]. Figure 1.1 shows both the historical data (up to 2004) and projections of the United States' energy consumption. The growing demand for fossil fuels, and petroleum in particular, will result in higher energy costs and greater reliance on imported oil given the current crude oil capacity. This can have a potentially negative impact on the nation's economic growth as rising commodity prices are closely tied to inflation rates. The combustion of fossil fuels contributes to increased levels of greenhouse gases which can have a severe environmental impact.

Renewable energy offers the opportunity to lessen fossil fuel consumption. Energy derived from solar, wind, hydroelectric, geothermal, and biomass sources are considered renewable. Because most forms of renewable energy are derived either directly or indirectly from the sun, there is an abundant supply of renewable energy available, unlike fossil fuels. The use of renewable energy also provides environmental, economic and political benefits.

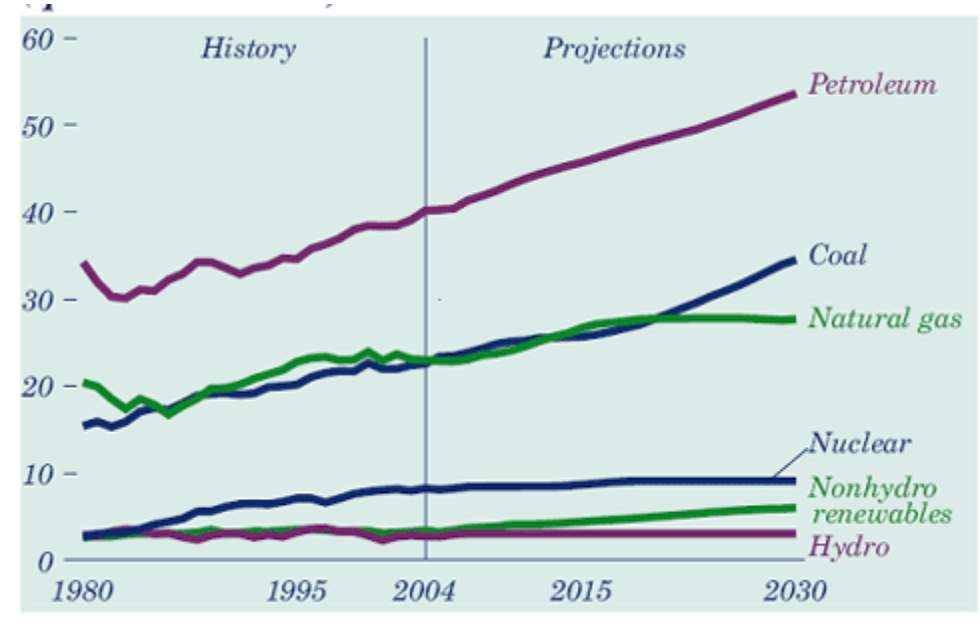

Figure 1.1- Energy consumption by fuel, 1980-2030 (quadrillion BTUs)[1]

The scope of the work discussed in this thesis pertains to energy derived from biomass, specifically, hydrogen gas. Biomass energy encompasses a broad category of energy derived from plants and animals as well as the residual materials from each. Hydrogen gas is an effective energy carrier which burns cleanly producing water as the only product. Hydrogen produced from a renewable source such as biomass provides a domestically available, CO_2 neutral, non-polluting form of energy.

1.2 HYDROGEN

Hydrogen is the most abundant element on the Earth. While not commonly found in nature, molecular hydrogen (hydrogen gas, H_2) can be produced from a wide variety of domestic resources using a number of different technologies. Having the highest energy content on a mass basis, hydrogen can be used as a storage medium. Hydrogen can also be used in combustion processes and fuel cells to provide a broad range of energy services.

1.2.1 Benefits of Hydrogen

The widespread use of hydrogen in this country could address issues concerning energy security and air quality. When combined with fuel cell technology, hydrogen offers the following benefits:

- **Strengthen National Energy Security:** By utilizing hydrogen in addition to other alternative energy sources, the United States can reduce its oil imports. The

U.S. uses 20 million barrels of oil per day and, according to the DOE, the use of biomass can reduce that amount by 30%.

- **Reduce Greenhouse Gas Emissions:** When hydrogen is produced from renewable sources such as biomass, there is no net increase in CO_2 emissions.
- **Reduce Air Pollution:** The combustion of fossil fuels from electric power plants and vehicles is responsible for most of the smog and harmful particulates in the air. Fuel cells powered by pure hydrogen emit no harmful pollutants.
- **Improve Energy Efficiency**: Fuel cells are significantly more energy efficient than combustion-based power generation technologies. A conventional combustion-based power plant typically generates electricity at efficiencies of 33 to 35 percent, while fuel cell plants can generate electricity at efficiencies of up to 85 percent, when fuel cells are used to generate electricity and heat (co-generation).

1.2.2 Limitations of Hydrogen

While hydrogen presents an attractive alternative to fossil fuel, there are several economic barriers and technical challenges to overcome before the "Hydrogen Economy" can become a reality.

1.2.2.1 Production and Infrastructure Costs

Approximately 95% of the hydrogen produced today is done so by steam reforming natural gas. This method of production is more expensive compared to conventional fossil fuels. To realize the benefits of using hydrogen to become more

energy independent, hydrogen would need to be produced from a variety of sources. By producing hydrogen from natural gas, the environmental benefits are also lost as CO_2 is still the main byproduct. Developing technologies that utilize renewable sources such as biomass can address some of these issues.

Another cost barrier to hydrogen utilization is the lack of infrastructure. While hydrogen gas has the highest energy content on a mass basis, it has one of the lowest on a volume basis. This makes transportation and distribution of hydrogen difficult and costly. Several distribution scenarios have been proposed ranging from "centralized production" (large production facility with distribution network) to a "distributed production" (several smaller spread out production facilities) and everything in between. As hydrogen production technology develops, hydrogen feed stock availability may dictate how the infrastructure pans out.

1.2.2.2 Fuel Cell and Storage Technology

Currently fuel cells offer the most efficient use of hydrogen energy. However, precious metal catalysis and proton exchange membrane (PEM) materials contribute to the high costs of fuel cells. There are other technical barriers, including durability, temperature resistance, and catalyst poisoning, which are being addressed with ongoing research. Because hydrogen has such a low energy density on a volume basis, effective storage must be developed. Research is currently being performed on metal hydrides and nanostructures as possible solutions to optimize storage [2].

1.3 RESEARCH OBJECTIVES

The goal of the work presented in this thesis was to develop two different methods to produce hydrogen gas using biomass as a renewable energy source. The first method was to produce hydrogen using photosynthetic algae. *C. reinhardtii* has been shown to produce hydrogen using light as an energy source. The objective of this work was to increase hydrogen production by a) manipulating process variables such as cell concentration, light intensity, and reactor design and b) immobilizing the algal cells to increase photosynthetic efficiency and address production limitations.

The second method of hydrogen production explored was gasification of biomass using supercritical water. A continuous SCW reactor was constructed to increase capacity and understand the optimum conditions necessary to gasify model compounds. Increasing the capacity of SCW reactors and understanding how basic components of biomass react may lead to further development of this technology.

1.4 REFERENCES

1. Annual Energy Outlook 2006 with Projections to 2030. Energy Information Administration Report #:DOE/EIA-0383(2006)

2. DOE Hydrogen Program: 2005 Annual Progress Report

2 *Chlamydomonas reinhardtii* LITERATURE REVIEW

2.1 INTRODUCTION

Biological methods of producing hydrogen gas (H_2) provide the advantage of having the ability to efficiently harness the low-density solar energy readily available at the surface of the Earth. The annual energy available from sunlight is estimated at 4 x 10^{24} J while the energy available from all supply of fossil fuel sources is estimated at 3 x 10^{24} J [1]. While photovoltaic cells can harness energy more efficiently, photosynthetic plants and micro organisms have the ability to grow and collect energy on their own. From a thermodynamic perspective, biological systems can potentially collect low density, or high entropy, sunlight and convert it to a lower entropy, usable, energy source [2]. This chapter will discuss some of the methods available to produce hydrogen, including the use of photosynthetic algae.

2.2 BIOLOGICAL HYDROGEN PRODUCTION

2.2.1 Photosynthesis

Photosynthesis occurs in the chloroplasts of plant cells. In essence, these chloroplasts contain reaction centers, known as photosystems, which use light photons to create electron reducing potential. A simplified schematic of the photosynthesis process

is shown in Figure 2.1. Photosystem II (PS II) excites the electrons transferred from a water molecule, essentially splitting it to form oxygen gas (O_2) which then cascades through a series of reactions. The cascade of reactions creates a proton gradient across the thylakoid membrane which houses these reaction centers. The proton gradient drives the ATP synthase protein to generate adenosine triphosphate (ATP), an energy medium used in living organisms. Photons excite electrons in Photosystem I (PS I) which then works in tandem with ferredoxin (Fd), a water soluble protein containing a Fe-S cluster. The ferredoxin is used to reduce NAP^+ to NADPH, in essence another form of energy currency used in biological systems. The net result is a conversion of:

$$H_2O + \text{Light} \rightarrow O_2 + ATP + NADPH \qquad \text{Eq. 2.1}$$

In photosynthetic plants, NADPH and ATP are used to reduce CO_2 and drive the reaction processes to build hexoses and other organic materials. Plants lack the hydrogenase enzyme, present in green algae and cyanobacteria, which can catalyze the reduction of protons to H_2 under specific conditions [3].

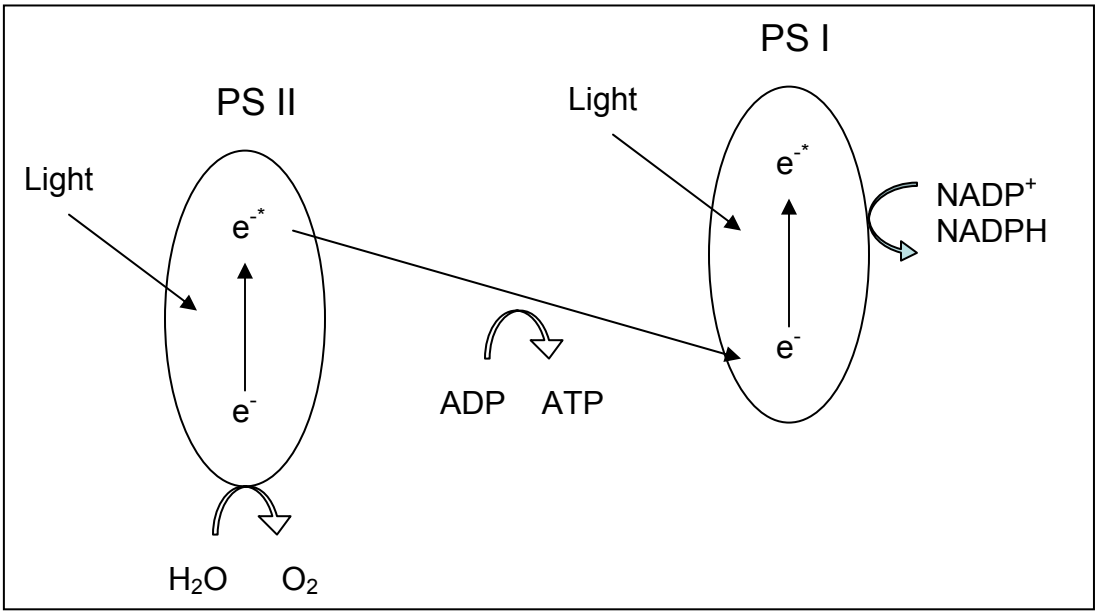

Figure 2.1- Photosynthesis process showing the two Photosystems (PS I and PS II) involved in splitting water and the production of ATP and NADPH.

2.2.2 Photosynthetic Bacteria

Cyanobacteria or blue-green algae are classified as nitrogen fixing bacteria. Photosynthetic strains of bacteria employ the same type of photosynthesis seen in higher plants. Under normal circumstances, nitrogenase enzyme catalyzes the reduction of nitrogen gas (N_2) to ammonia (NH_3). In the absence of N_2, nitrogenase can also facilitate the production of H_2. Many researchers have studied the nitrogenase system for H_2 production [4-7] and have developed various mechanisms. There is some disagreement on which nitrogenase metal centers are active and whether hydrogenase facilitates part of the reaction. Most researchers do believe the nitrogenase facilitated reaction requires ATP input as shown in Eq. 2.2.

$$2H^+ + 2Fd_{red} + 4ATP \xrightarrow[N_2ase]{} H_2 + 2Fd_{ox} + 4ADP + Pi \qquad \text{Eq 2.2}$$

For this reason, Lee *et. al.* [7] concludes green algae would be better suited for H_2 production since green algae does not require the same high energy input of the nitrogenase enzyme.

2.2.3 Photosynthetic Algae

Photosynthetic production of H_2 from green algae was first observed by Gaffron and Rubin in 1942 [8]. After a period of dark anaerobic incubation, algal cells were able to photoproduce H_2. The reversible production of H_2 is catalyzed by the hydrogenase enzyme [9] coupled with ferredoxin (Fd) as shown in Eq. 2.3.

$$2H^+ + 2Fd_{red} \xleftrightarrow{H_2ase} H_2 + 2Fd_{ox} \qquad \text{Eq 2.3}$$

Unlike the bacterial cells which utilize nitrogenase, hydrogenase does not require ATP to catalyze the reduction of protons to make H_2. However, the presence of O_2 can quickly deactivate the hydrogenase enzyme within a matter of minutes [10, 11]. As a result, sustainable H_2 production is difficult without additional measures to either deactivate PS II activity or separate/scavenge O_2.

2.2.4 Fermentative Hydrogen Production

Fermentation of organic compounds has not received much attention compared to photosynthetic production of H_2. However fermentation does present certain advantages [12]:

- Fermentative bacteria have high evolution rate of H_2
- H_2 production does not require light
- Fermentative bacteria can readily grow for production

Under anaerobic conditions, organic materials are oxidized and the excess electrons are used to produce H_2, facilitated by the hydrogenase enzyme [13,14]. A second mechanism for hydrogen production occurs when NADH is formed through glycolysis (conversion of glucose to pyruvate). NADH is then oxidized [15]:

$$NADH + H^+ \rightarrow H_2 + NAD^+ \quad \text{Eq. 2.4}$$

Increased CO_2 levels produced from the fermentation process elevates levels of succinate and formate which in turn reduce the yield of H_2. In order to sustain H_2 production, CO_2 must be removed, which can add expense to the process. The breakdown of organic materials requires additional glucose to act as "fuel" for the bacteria which can also add expense.

2.3 CHLAMYDOMONAS REINHARDTII

2.3.1 Chlamydomonas Background

Chlamydomonas is a genus of unicellular green algae. Algae in this genus have a cell wall, a chloroplast, and two anterior flagella for motion. More than 500 different species of Chlamydomonas have been described, but most scientists work with only a few. The most widely used laboratory species is *Chlamydomonas reinhardtii.* Cells of this species are haploid, and can grow on a simple medium of inorganic salts, using photosynthesis to provide energy. They can also grow in total darkness if acetate is provided as an alternative carbon source [16].

Chlamydomonas is used as a model system for research in cell and molecular biology. When yeast cells cannot be used, chlamydomonas is used to approach genetic or molecular aspects of [17]:

- Photosynthesis
- Motility and Phototaxis
- Flagella
- Centrioles and Basal Bodies
- Chloroplast Biogenesis and Inheritance

2.3.2 Biophotolysis and Chlamydomonas

Because the hydrogenase enzyme found in *Chlamydomonas reinhardtii* is sensitive to O_2, O_2 removal or separation is critical in order to sustain H_2 production. Methods have included the use of oxygen scavengers [18, 19], reductants [19], and purging with inert gases [20, 21]. Due to the added costs and potential death of the cells, these measures may not be economically feasible for H_2 production.

Another approach to address oxygen sensitivity is to separate the formation of O_2 and H_2 in the photosynthetic process. When *Chlamydomonas reinhardtii* cells are deprived of sulfur, PS II activity is reduced, significantly reducing the evolution of O_2 [22]. The remaining oxygen is consumed in normal cellular respiration. Within a period of 24 hours, the environment becomes anaerobic. Figure 2.2 shows the levels of dissolved O_2 and H_2 produced by a *Chlamydomonas reinhardtii* culture once sulfates were removed from the medium. Hydrogen production begins soon after all the oxygen is consumed by the cells. Once the hydrogen production phase concludes, sulfates can be re-introduced to the cell cultures and normal cell growth and activity resumes [23]. This cycle can continue indefinitely, with the addition and removal of sulfates to switch between production and growth modes, respectively, as shown in Figure 2.3.

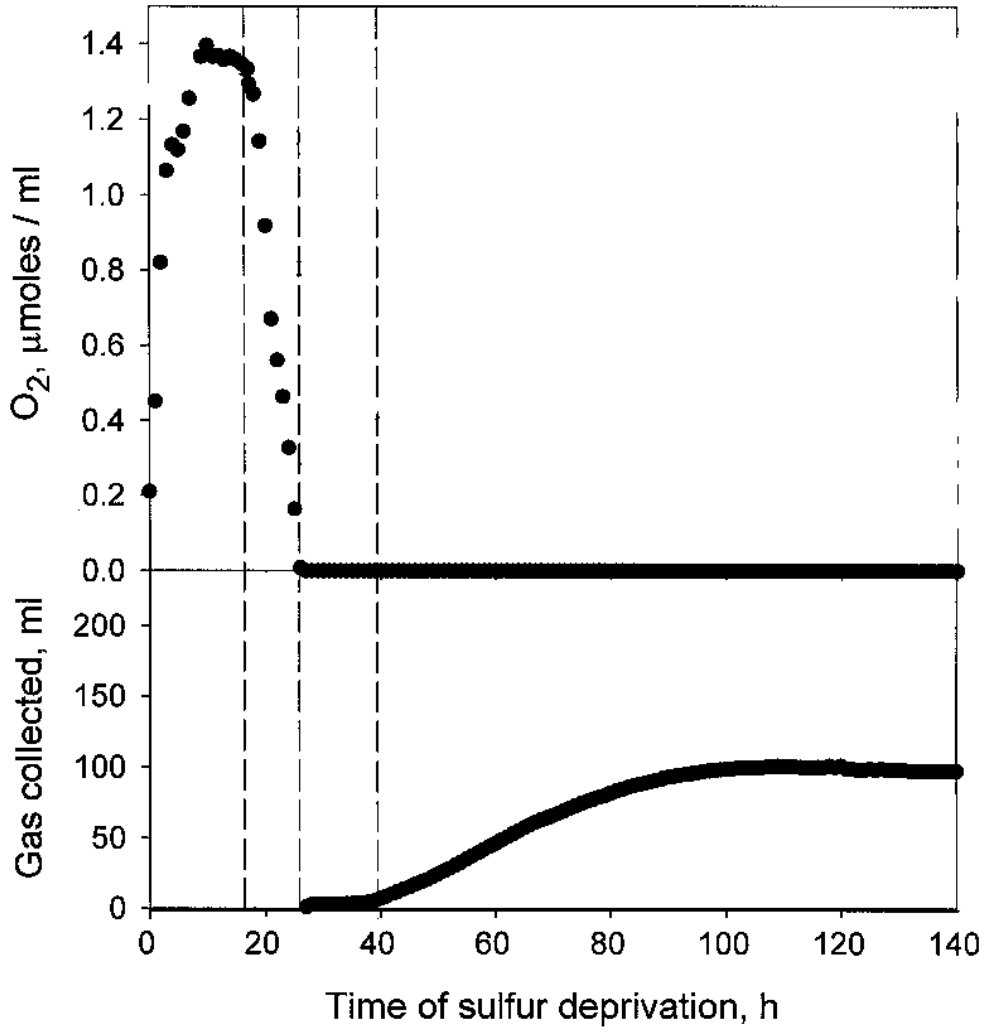

Figure 2.2- Plot of dissolved O_2 and H_2 produced as a function of time once the *Chlamydomonas reinhardtii* cells are deprived of sulfates.

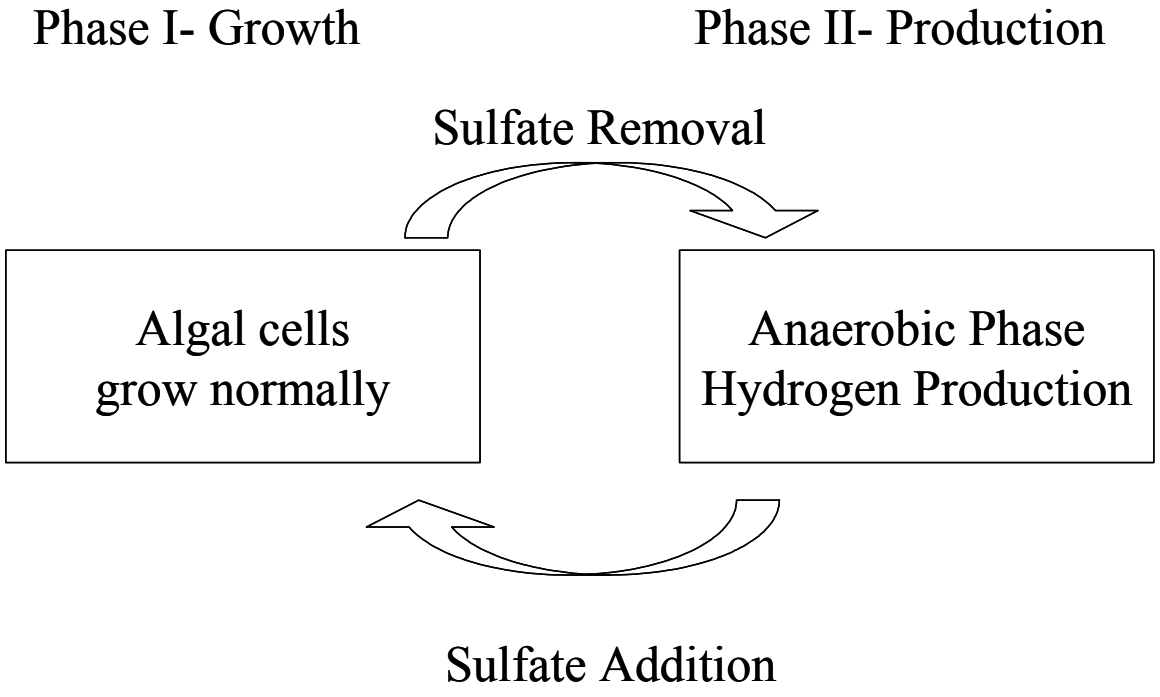

Figure 2.3- Diagram showing alternating growth and production phases with the removal and addition of sulfates to the algal cell culture.

2.4 SUMMARY

Photosynthesis offers a method to harness the power of the sun to produce hydrogen gas. Unlike conventional methods of reforming natural gas, photosynthesis utilizes a virtually unlimited source of energy which has the added benefit of being CO_2 neutral. The use of *Chlamydomonas reinhardtii* has been shown to be the most feasible method of photosynthetically producing H_2 gas to date, but the overall yields are too low and expensive processing steps make using green algae economically unattractive.

2.5 REFERENCES

1. Miyake, J. The Science of Biohydrogen: An Energetic View. *BioHydrogen*, [Proceedings of an International Conference on Biological Hydrogen Production], 1997.

2. Rifkin, J. Entropy. Bantam Books, NY. 1981.

3. Benemann JR. Feasibility analysis of photobiological hydrogen production. *Int J Hydrogen Energy*. 1997 22:979-87.

4. Gogotov IN. Relationships in hydrogen metabolism between hydrogenase and nitrogenase in phototropic bacteria. *Biochimie*. 1978, 68:181-186.

5. Rao KK, Hall DO. Hydrogen production by cyanobacteria: potential, problems and prospects. *J Mar Biotechnol.* 1996, 4:10-15.

6. Tsygankov AA, Borodin VB, Rao KK, Hall DO. H_2 photoproduction by batch culture of *Anabaena variabilis* ATCC 29413 and its mutant PK84 in a Photobioreactor. *Biotech Bioeng.* 1999, 64:709-715.

7. Lee, JW, Greenaum, E. A new perspective on hydrogen production of photosynthetic water splitting. *Fuels and chemical for biomass, ACS Symposium Series,* Washington: ACS. 666, 1997, 209-222.

8. Gaffron H, Rubin, J. Fermentative and photochemical production of hydrogen in algae. *J Gen Physiol*. 1942, 26:219-240.

9. Boichenko, VA, Hoffmann, P. Photosynthetic hydrogen production in prokaryotes and eukaryotes: occurrence, mechanism, and functions. *Photosynthetica.* 1994, 30: 527-552.

10. Ghiardi ML, Togasaki RK, Seibert M. Oxygen sensitivity of algal H_2 production. *Appl Biochem Biotech*. 1997, 63: 141-151.

11. Benemann JR, Berenson JA, Kaplan NO, Kauren MD. Hydrogen evolution by a chloroplast-ferredoxin-hydrogenase system. *Proc Natl Acad Sci USA*. 1973, 70: 2317-2320.

12. Das D, Veziroglu TN. Hydrogen production by biological processes. *Int. J Hydrogen Energy.* 2001, 26:13-28.

13. Tanisho S, Suzuki Y, Wakoo N. Fermentative hydrogen evolution by *Enterobacter aerogenes* strain E.82005. *Int J Hydrogen Energy.* 1987, 12: 623-627.

14. Woodward J, Orr M, Corday K, Greenbaum E. Enzymatic production of biohydrogen. *Nature*. 2000, 405: 1014-1015.

15. Tanisho S, Kuromoto M, Kadokura N. Effect of CO_2 removal on hydrogen production by fermentation. *Int J Hydrogen Energy.* 1998, 35:559-563.

16. Harris, EH. Chlamydomonas as a model organism. *Annual Review of Plant Physiology and Plant Molecular Biology*. 2001, 52:363-406.

17. Lefebvre, PA and Silflow, CD. Chlamydomonas: The cell and its genomes. *Genetics.* 1999, 151:9-14.

18. Healy FP. The mechanism of hydrogen evolution by *Chlamydomonas moewusii*. *Plant Physiol*. 1970, 45:153-159.

19. Randt C, Senger H. Participation of the two photosystems in light dependent hydrogen evolution in *Scenedesmus obliquus. Plant Physiol.* 1985, 42:553-557.

20. Greenbaum E. Photosynthetic hydrogen and oxygen production: kinetic studies. *Science.* 1982, 196:879-880.

21. Gfeller RP, Gibbs M. Fermentative metabolism of *Chlamydomonas reinhardtii*, I: Analysis of fermentative products from starch in dark and light. *Plant Physiol.* 1984, 75:212-218.

22. Melis A, Zhang L, Forestier M, Ghirardi ML, Siebert M. Sustained photobiological hydropgen gas production upon reversible inactivation of oxygen evolution in the green algae *Chlamydomonas reinhardtii. Plant Physiol.* 2000, 122:127-135.

23. Ghirardi ML, Zhang L, Lee JW, Flynn T, Seibert M, Greenbaum E, Melis A. Microalgae: a green source of renewable H_2. *Trends Biotechnol.* 2000, 18:506-511.

3 OPTIMIZATION OF PROCESS VARIABLES FOR ALGAL PHOTOPRODUCTION OF HYDROGEN

3.1 INTRODUCTION

Photosynthetic bacteria, cyanobacteria and green algae produce hydrogen gas (H_2) using energy from the sun. Photosynthetic bacteria and cyanobacteria rely on the nitrogenase enzyme to mediate this process [1-3]. In the case of green algae, the production of hydrogen depends on the reversible [Fe]-hydrogenase enzyme, which directly catalyzes the reduction of protons to hydrogen gas [4]. Unlike the nitrogenase system, the hydrogenase does not require energy (in the form of ATP) to mediate the reaction.

In green algae, H_2 photoproduction is initiated by the photosynthetic water-splitting process of Photosystem II (PS II) and subsequent transport of electrons from water to ferredoxin through Photosystem I (PS I). Reduced ferredoxin, in turn, reduces protons in a reaction catalyzed by the reversible hydrogenase enzyme. This process results in the simultaneous release of both oxygen gas (O_2) and H_2 with a maximum theoretical H_2 to O_2 ratio of 2 to 1 on a molecular basis [5]. The reversible hydrogenase in green algae is highly sensitive to O_2, which irreversibly inactivates the enzyme's activity within minutes [6]. Therefore, this is not a sustainable path for hydrogen production. However, Melis *et al*. [7] and Ghirardi *et al*. [8] recently proposed a mechanism to partially inactivate PS II activity to a point where all the O_2 evolved by

photosynthesis is immediately taken up by the respiratory activity of the culture. This mechanism is based on sulfur deprivation from the culture medium, and results in a temporal separation of net O_2- and H_2-evolution activities in the green alga *Chlamydomonas reinhardtii*. During the first phase, O_2 evolution in the presence of a complete growth medium, the algae photosynthesize and accumulate starch. In the second phase, H_2-photoproduction is initiated after transfer of the culture to a sulfur-deficient medium. The O_2-evolution activity of the cells is gradually inactivated, and the culture becomes anaerobic due to respiratory oxidation of starch. After about 24 hours, H_2 production commences and proceeds for up to four days. At this point, the culture may be recycled back to the first phase by re-adding sulfate and the process can be repeated many times [8].

This process for H_2 production has received considerable attention in the last two years. Despite the publicity, reported hydrogen production rates are low and the process is not yet commercially viable [9]. However, the rates of H_2 photoproduction could potentially be increased by a factor of about ten by fulfilling the maximum capacity of the sulfur-deprived cultures to photosynthetically split water and generate reductants [7,10]. Other factors may affect the rates of H_2 production by sulfur-deprived cultures. For example, it has been reported that at high cell density, algal productivity is limited by light attenuation in the photobioreactor due to shading effects of the layers of cell closer to the surface [11,12]. Kosourov *et al*. [13] showed that the yields, or total output of H_2, increase but the specific rates of H_2 photoproduction by the system, measured on a volume basis, decrease as a function of light intensity. We investigated the effects of the

variables cell concentration, light intensity, light transport, and culture mixing on H_2 production by sulfur deprived cultures during one production cycle (approximately 96 hours). The response optimized in our experiments is specific H_2 production (ml H_2 produced at atmospheric pressure per ml of suspension). These units are appropriate for engineering scale-up and economic analysis of the process.

3.2 EXPERIMENTAL SETUP

3.2.1 Cell Growth

Cultures of *Chlamydomonas reinhardtii* were obtained from the National Renewable Energy Laboratory (NREL) on agar plates. The strains were transferred to a tris-acetate-phosphate (TAP) growth media. The TAP solution was made up of 0.242 wt% Trizma base (Sigma), 2.5 v% TAP salts (6 g/400ml NH_4Cl, 1.6 g/400ml $MgSO_4$, 0.6 g/400ml $CaCl_2 \cdot 2H_2O$), 0.0375v% phosphate buffer (28.8 wt% K_2HPO_4, 14.4 wt% KH_2PO_4), 0.1 v% Hutner's trace elements, and 0.1 v% glacial acetic acid [14]. All procedures were carried out under sterile conditions using a laminar flow hood whenever possible. The growth media and all glassware were autoclaved before use. The cultures were continuously illuminated from two sides with parallel sets of light banks. Each light bank was made up of four 15-watt cool-white fluorescent lights mounted horizontally. A 5% CO_2 in air gas mixture was used to aerate the cultures. The gas mixture was purified using a 0.2 μm membrane filter (Acro 37 TF, Gelman Sciences).

3.2.2 Concentration Determination

The cell density was determined by measuring chlorophyll concentration using ultraviolet/visible absorption spectroscopy, as described in Kosourov *et al*. [13]. A 1 or 2 ml sample of the suspension was collected, based on the density. The suspension was centrifuged for 2 minutes using a table top centrifuge to pellet down the cells. The supernatant was discarded, leaving behind the pellet of algal cells. A volume of 95% ethanol (typically 2 ml) was added to the centrifuge tube to resuspend the cells. The sample was centrifuged again for 2 minutes. The supernatant was poured into a cuvette and the absorbance at 649, 665, and 750 nm was measured using 95% ethanol as a blank. The chlorophyll concentration (μg/ml) was determined by the following formula:

$$\text{ChL Conc} = [6.10\,(A_{665} - A_{750}) + 20.04\,(A_{649} - A_{750})] \times [\text{dilution factor}] \quad \text{Eq 3.1}$$

$$[\text{dilution factor}] = [\text{ethanol vol. (ml)}] / [\text{suspension vol. (ml)}] \quad \text{Eq 3.2}$$

3.2.3 Cell Collection

When the algal concentration reached approximately 5×10^6 cells/ml, the transition from the aerobic growth phase to the anaerobic hydrogen production phase was made. The cells were separated from the TAP growth media via centrifugation (2000 *g* x 5 min). In order to make the cells sulfate free, the cells were washed in TAP-minus-sulfur (TAP-S) medium. The cells were washed by re-suspending the cells in TAP-S

medium followed by centrifugation. This procedure was repeated 3 times to remove any sulfates from the suspension. Finally, the cells were re-suspended in TAP-S medium at the specified concentrations.

3.2.4 Reactor Fabrication

Initial studies of hydrogen production were carried out in Erlenmeyer flasks. When set up on a magnetic stir plate, these flasks provide a method of even mixing, light transmission, and a gas tight set-up. While this setup was convenient, it was not possible to control the sample volume, amount of light transmitted, and path length (thickness of the reactor) independently.

Cylindrical reactors were fabricated from borosilicate tubing (4" OD) cut to 0.5 and 1.4 inch lengths. The ends of the tubing were sealed with borosilicate glass plates. A port was also fabricated out of 0.5" glass tubing on the top for loading and gas output (Figure 3.1a). All glass work was done at either the MU glass shop or Ray Allen glass works (Denver, CO).

a) 

b) 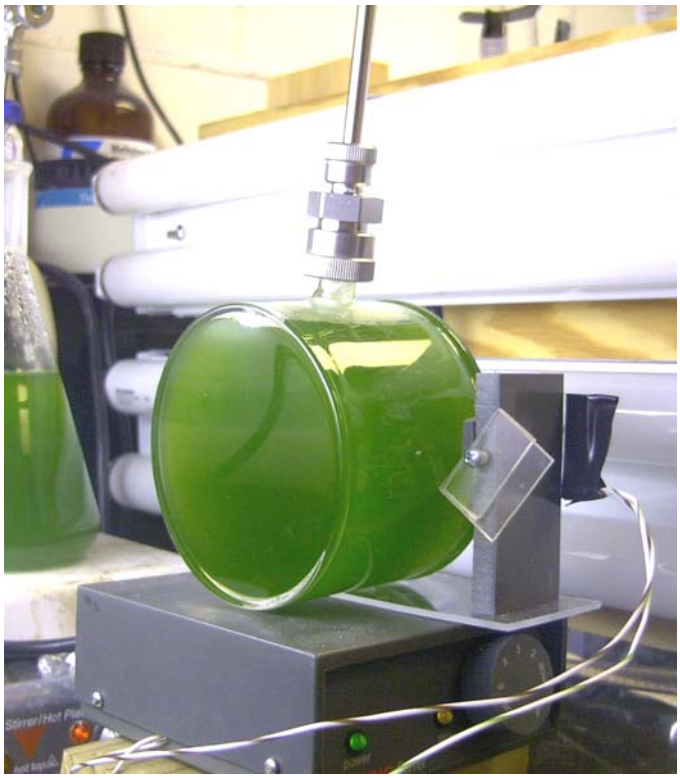

Figure 3.1- Photobioreactor. (a) Conventional Erlenmeyer. (b) Cylindrical.

3.2.5 Gas Collection

All the reactors were attached to manometers to measure hydrogen gas output from the algae in the system. One-quarter inch stainless steel tubing and glass were used to minimize any gas leaks. The pressure reading from the manometer was converted into change of volume produced or consumed.

After the reactor was sterilized by autoclave (121°C, 14 psig, 15 min), it was loaded with the algae suspension washed with TAP-S medium. The suspension equilibrated for 24 hours in the light banks at the specified light intensity. After 24 hours, the head space in the reactor was purged with nitrogen for 1 minute and the reactor was sealed and connected to the manometer. For the next 24 hours, the algae consumed dissolved oxygen, and the system became anaerobic, indicated by a drop in pressure. The cells then enter the production phase and produce H_2 gas for the next 4 days. The total cumulative volume of gas produced was recorded. Because maximizing the H_2 output was the objective of this work, the measured response was also recorded as total volume of H_2 produced per volume of algal suspension for the 4-day cycle.

3.3 EXPERIMENTAL DESIGN

3.3.1 Design of Experiments

In order to evaluate a large number of factors that may affect gas production, a 2-level screening design was used to determine the statistical significance of each factor. A low resolution was used to determine the main effects without any knowledge of

interaction between the factors. The significant effects were then individually studied in more detail. Discussion on statistically designed experiments was described by Box *et al*. [15].

3.3.2 $2^{(6-3)}$ Design

Using the Erlenmeyer and glass cylindrical reactors that were constructed, a screening experiment was set up to study the effects shown in Table 3.1. This table also shows both the low and high levels used in the experiment. Table 3.2 shows the aliasing structure.

The light intensity was adjusted by changing the distance of the light banks from the reactor. The reactor comparison was made using the cylindrical plastic reactors and Erlenmeyer flasks of comparable volume. The temperature was controlled using a fan to cool the heat generated by the lamps. The agitation was set by adjusting the stir plate to the lowest and highest setting.

Table 3.1- List of effects tested and levels studied in screening experiment.

Factor	Low Level (-)	High Level (+)	Units
Light	100	150	$\mu E \bullet m^{-2} \bullet s^{-1}$
Reactor	Erlenmeyer	Plas. Cyl.	
Volume	90	240	ml.
Temperature	26	32	°C
Algae Conc.	15	30	μg Chl/ml
Agitation	Slow	Fast	

Table 3.2- Aliasing structure

Effect	Alias 1	Alias 2
Light	Volume*Agitation	Temp*Conc
Reactor	Volume*Conc	Temp*Agitation
Volume	Light*Agitation	Reactor*Conc
Temp	Light*Conc	Reactor*Agitation
Algae Conc.	Light*Temp	Reactor*Volume
Agitation	Light*Volume	Reactor*Temp
Light*Reactor	Volume*Temp	Conc*Agitation

3.3.3 Individual Effect Experiments

The goal of this work was to increase hydrogen production rates by manipulating process variables. Inferences about two such variables, light transport and mixing, were made based on data taken with two types of reactors, Erlenmeyer flask and glass cylindrical design. Each of the reactor designs was executed in several different sizes (volumes), light intensity, and concentration; this changed the light path length and the flux of light. The first of two reactor designs was an Erlenmeyer flask with a 24/40 ground-glass fitting. Two different sizes were used, 125 ml and 250 ml. Specifications of the flask reactors are shown in Table 3.3. This table shows the volume of algal suspension held and two different surface areas. The first was the interfacial surface area, the total area of the glass that was in contact with the suspension. The second was the normal surface area, the amount of glass that was normal to the incident light (the profile of the flask).

The second type of reactor was designed for improved light transport and mixing characteristics relative to the Erlenmeyer flask reactors. Table 3.3 also shows the dimensions of the cylindrical reactors used in the experiments. Once again, two surface areas, interfacial and normal, are reported for the cylindrical reactors. Varying the axial thickness of the cylinder made cylindrical reactors of various volumes and light path lengths. The smaller reactor, with a 1.7 cm axial thickness, held 125 ml of suspension while the larger reactor (axial thickness = 3.1 cm) reactor held 220 ml of suspension. This facilitates comparison with the Erlenmeyer flask reactors, which have the same volumes. A third cylindrical reactor was fabricated with an axial length of 6.1 cm, which held 440 ml of suspension.

Table 3.3- Specifications of the reactors used in the experiments.

Reactor type	Volume of suspension held (ml)	Surface area normal to light (cm^2)	Path Length (cm)	Normal Surface area/volume ratio (cm^{-1})
125 ml Flask	125	60	3.6	16.6
250 ml Flask	220	90	4.6	19.8
1.7 cm Cylinder	125	139	1.7	1.11
3.1 cm Cylinder	220	139	3.1	0.63
6.1 cm Cylinder	440	139	6.2	0.32

3.4 RESULTS

3.4.1 Factorial Results

The results of the factorial experiments are shown in Table 3.4. The results are - presented as total hydrogen gas produced. Because one of the objectives of this experiment was to maximize hydrogen yield, the total hydrogen gas produced per volume of solution used in the reactor was also calculated. The response of each effect is shown at the bottom of the table. The response was calculated based on each output. The response of each factor was the mean change observed as the factor moved from the low level (-) to the high level (+). When these responses were compared to a normal distribution plot, two effects were found to have 3 times the magnitude of the others- light intensity and algal concentration. In other words, the remaining 4 effects did not change the output of hydrogen beyond the level of noise. However, the effect of volume must be singled out because while the total output of hydrogen increased with increasing reactor volume, the specific per volume output did not change, and therefore was not seen as significant in this test. Two-way interactions were not found to be significant.

Table 3.4- Results of fractional factorial with responses.

Run	Light	React	Vol	Temp	Conc	Agit	L*R	Total H_2 Prod. (ml)	ml H_2 per ml soln*cycle
1	-	-	-	-	+	+	+	29	0.322
2	-	-	+	+	-	-	+	50	0.208
3	-	+	-	+	-	+	-	17.5	0.194
4	-	+	+	-	+	-	-	58.5	0.244
5	+	-	-	+	+	-	-	22.5	0.25
6	+	-	+	-	-	+	-	25.7	0.107
7	+	+	-	-	-	-	+	10.4	0.112
8	+	+	+	+	+	+	+	54.5	0.227
Response- Total H_2	5.24	-1.71	-13.66	-2.61	-7.61	-1.84	-1.84		
Response- per Vol.	0.0336	0.0133	0.012	-0.0114	-0.0522	0.0041	0.0097		

When the data was analyzed with respect to the H_2 output per volume results, the volume effect was shown to be statistically insignificant. While this result may not seem unexpected, it was difficult to absolutely assess the volume effect. The shapes of the two types of reactors are quite different and allow differing amounts of light to be transmitted. The volume term in this set of experiments does not take into consideration the depth, or path length, the light has to penetrate in the reactor.

3.4.2 Concentration results

After the initial screening experiments, a more thorough investigation of the effects of light intensity and algal concentration was carried out. The hypothesis, increasing the cell concentration of cultures under sulfur deprivation leads to increased hydrogen production, was tested.

The concentration experiments were performed using the 250 ml Erlenmeyer flask reactors containing 220 ml of cell suspension. The light intensity was 100 $mE \bullet m^{-2} \bullet s^{-1}$ PAR. Figure 3.2 shows the total yield of hydrogen production as a function of the initial cell concentration. The abscissa is algal density as measured by chlorophyll concentration. The ordinate is cumulative hydrogen production over the entire productive period reported on a volume basis. The error bars represent the 95% confidence interval for that population to provide an indication of the variability in the data.

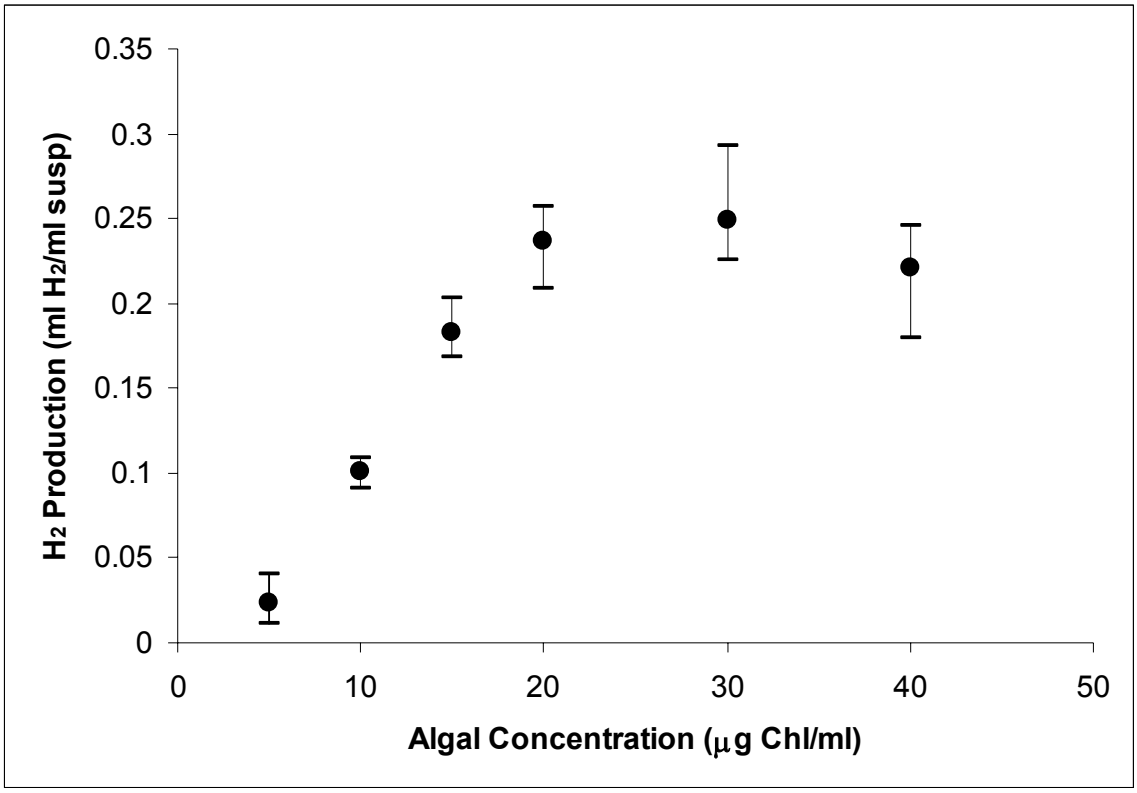

Figure 3.2- Total yields of H_2 photoproduction (in ml) as a function of cell density (measured as Chl concentration, mg/ml) in Erlenmeyer photobioreactors. Each experiment lasted 5 days.

At low concentrations, the production of hydrogen gas is linearly proportional to the cell concentration. Once the cell concentration reaches about 20 mg Chl/ml, hydrogen production saturates and the yields become independent of further changes in cell concentration. The total yields reported in Figure 3.2 closely agree with those reported by Kosourov *et al*. [13]. One possible explanation for hydrogen production becoming independent of cell concentration above 20 mg Chl/ml is the faster accumulation of products of dark anaerobic fermentation (e.g., acetate and formate) that lead to a drop in the pH of the medium, inactivating photosynthesis.

3.4.3 Light intensity results

Another explanation for the behavior observed in Section 3.4.2 is that, in the 250 ml Erlenmeyer flask reactors, light transport limits hydrogen production in cultures above 20 mg/ml chlorophyll. This hypothesis was tested by varying the light intensity for suspensions containing 30 mg Chl/ml. These experiments were also performed in the 250 ml Erlenmeyer flask reactors.

Figure 3.3 shows cumulative hydrogen production on a volumetric basis as a function of light intensity for two different concentrations. The open circles represent an algal concentration of 15 mg ChL/ml and the solid circles represent an algal concentration of 30 mg ChL/ml. At lower light intensities, the hydrogen production rates for both algal concentrations are almost identical. This would indicate the hydrogen output is limited by the amount of light. As the light intensity increases to 100 $\mu E \bullet m^{-2} \bullet s^{-1}$ PAR, both concentration levels reach a maximum hydrogen output before they both drop off significantly. At this higher light intensity, the system appears to be saturated with

light and the only limiting factor at this point is the algal concentration. It is difficult to understand why hydrogen production drops so sharply at 150 $\mu E \bullet m^{-2} \bullet s^{-1}$ PAR. These results are consistent with the factorial experiments where increased light was found to have a negative effect on hydrogen production. This decrease is also consistent with work done by Laurinavichene *et al* using immobilized algal cells [16]. Because the hydrogen production actually decreases instead of leveling off at higher light intensities, another reaction or set of reactions may be taking place to the detriment of the hydrogen production.

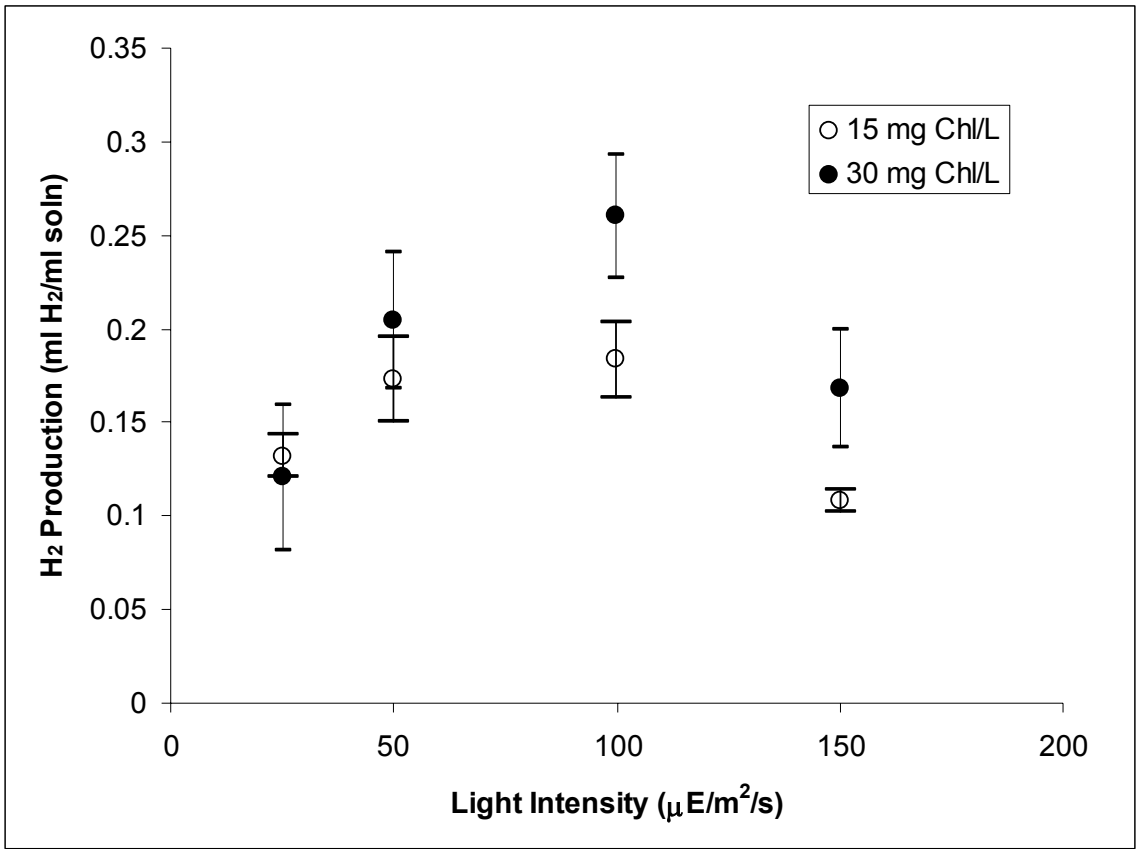

Figure 3.3- Total yields of H_2 photoproduction (in ml) as a function of incident light intensity ($\mu E \bullet m^{-2} \bullet s^{-1}$).

3.4.4 Path length results

Although the screening experiments did not show a significant difference in the two reactor designs, there was no way to isolate optical path length as an individual effect because this variable is fixed in the case of the Erlenmeyer flask reactors. When the data for the glass cylindrical reactors were separated from the Erlenmeyer reactor data, a potential interaction appeared between algal concentration and reactor volume (or path length in the case of the glass cylinders) which was not observed in the Erlenmeyer data.

To test the effect of path length, a thicker cylinder reactor was constructed with the same normal surface area and a longer path length of 6.2 cm. Experiments were carried out using two different concentrations, 15 mg Chl/ml and 30 mg Chl/ml, at a light intensity of 100 $\mu E \bullet m^{-2} \bullet s^{-1}$ PAR. Figure 3.4 shows the hydrogen production as a function of path length. Production, on a volumetric basis, increased when going from a path length of 1.7 cm to 3.1 cm, but the positive trend did not extend to a path length of 6.2 cm.

In order to understand the observed trend in Figure 3.4, the cylindrical reactors must be examined. The amount of incident light that enters the "system," defined as our reactor, is a function of light intensity and normal surface area. The cylindrical reactors make this determination very simple due to their geometry. However, once the light enters the system, its effectiveness in driving H_2 production will depend on cell concentration and path length. It is conceivable that, as we take a cylindrical reactor with a fixed normal surface area and extend the path length to 10, 20, or 100 cm, we

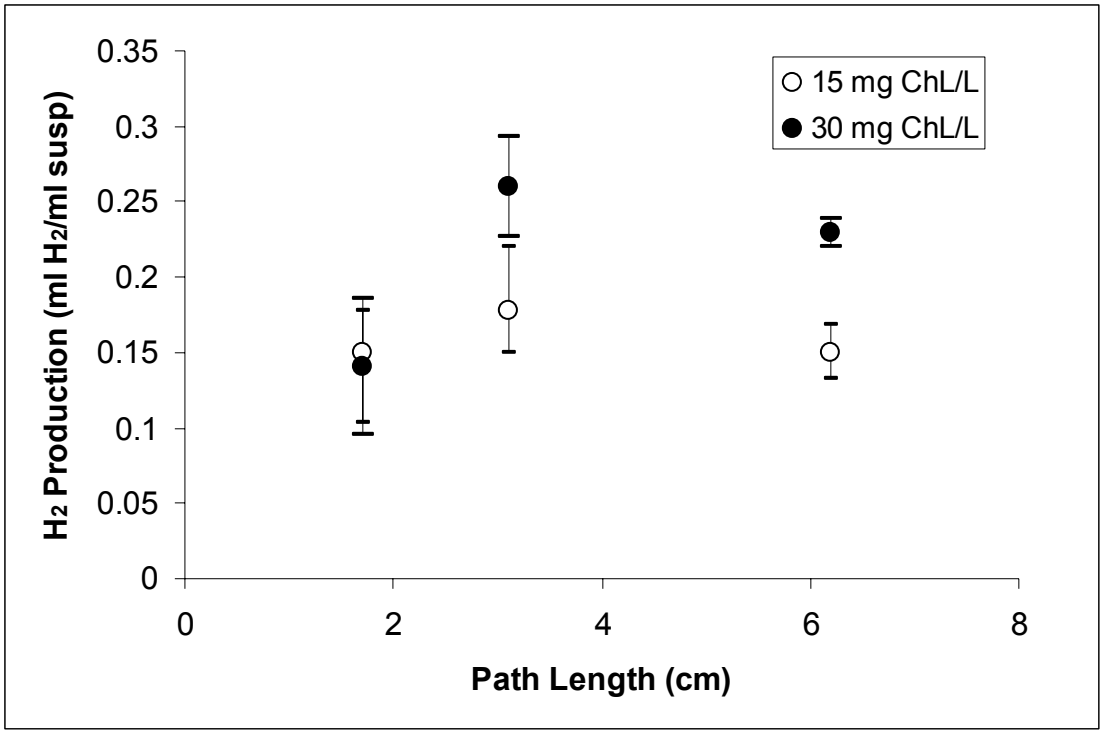

Figure 3.4- H_2 production as a function of reactor volume; the horizontal axis is the light reactor volume of the cylindrical reactors and the vertical axis is the H_2 production. Data for two concentrations are shown: 15 μg Chl/ml and 30 μg Chl/ml. The light intensity was 100 $\mu E \bullet m^{-2} \bullet s^{-1}$ PAR.

would observe a diminishing trend in specific hydrogen output due to the fixed number of incident photons being utilized by an increasing number of algal cells.

Using the dimensions calculated in Table 3.3, the data of Figure 3.4 was replotted in Figure 3.5 using the ratio of normal surface area to path length. As this ratio increases, the amount of light relative to the depth of the reactor increases. The trend seen in Figure 3.5 is similar to that seen in Figure 3.3. Both graphs show a light-limited range at low values, but as these levels increase, the same diminished effect on hydrogen output is observed due to the "overabundance" of light. This trend is consistent with the discussion of Section 3.4.3.

Four points representing average Erlenmeyer flask data are also shown in Figure 3.5 indicated as triangles. 125 ml and 250 ml Erlenmeyer flasks have corresponding SA/Path ratios of 16.6 and 19.8 cm, respectively, and are represented in the figure accordingly. A change in volume for the Erlenmeyer flask reactors does not significantly affect the surface area to path length ratio. This observation could explain why the same interaction between volume and algal concentration are not observed for this class of reactors. As the volume changes in the cylindrical reactors, the surface area to path length changes significantly, leading to substantial changes in the hydrogen output. Since both sets of Erlenmeyer flask reactors have very similar surface area to path length ratios, no significant change in output is observed.

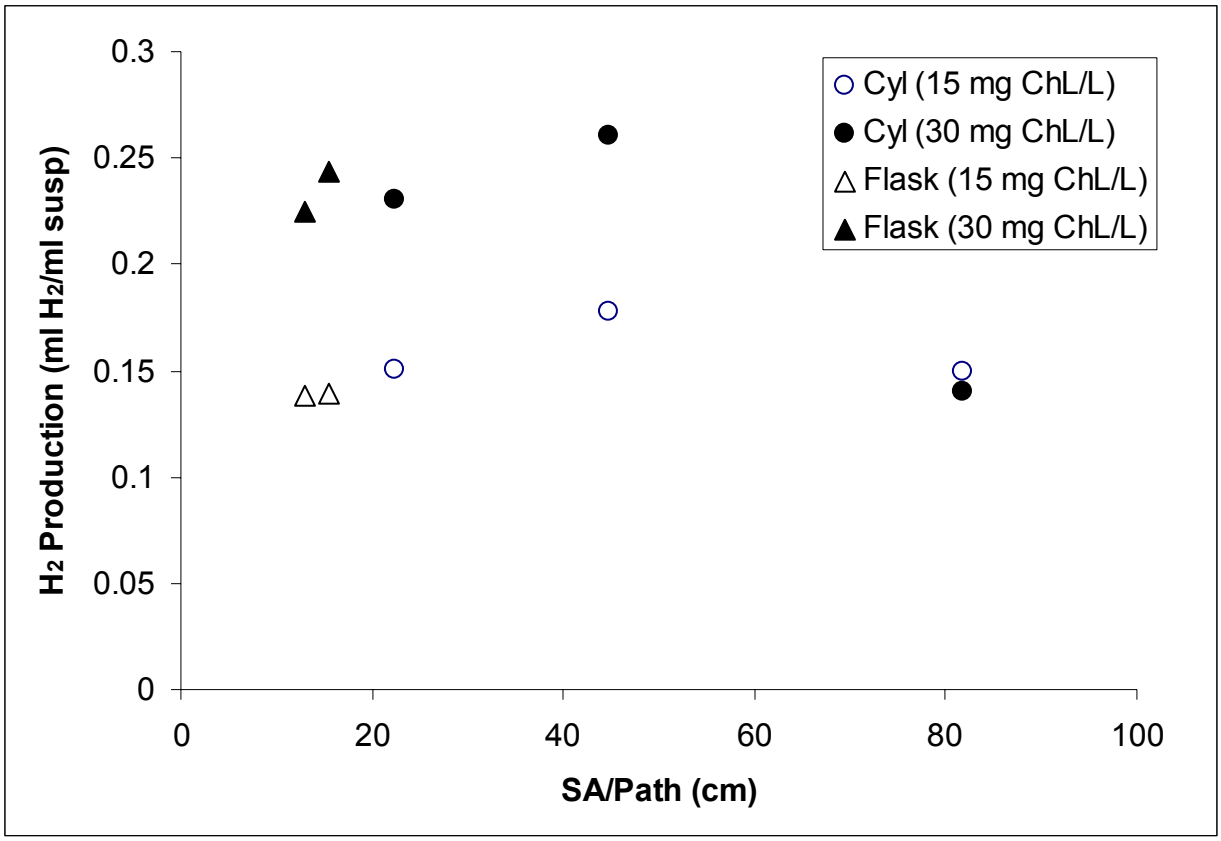

Figure 3.5- H_2 production as a function of normal surface area/path length. The light intensity was 100 $\mu E \bullet m^{-2} \bullet s^{-1}$ PAR. Data for the Erlenmeyer flask reactors are also shown for comparison.

3.5 CONCLUSIONS

The final yield of hydrogen gas was shown to be linearly proportional to the cell concentration at low concentrations, but above 20 μg Chl/ml, hydrogen yield is independent of this parameter. The production of hydrogen increases as light intensity increases and reaches a maximum at about 100 $\mu E \bullet m^{-2} \bullet s^{-1}$ PAR, then drops at higher light intensity, independent of the cell concentration. In relation to the light effect, we have identified a parameter, surface area to path length, which may be critical for scale up efforts. Due to low H_2 yield reported in this and other studies, future work must focus on understanding the mechanisms of *Chlamydomonas reinhardtii* and developing more productive and oxygen tolerant strains. At that point, these engineering parameters can be revisited with an eye toward optimization and scale up. These results have been published in a peer-reviewed journal [17].

3.6 REFERENCES

1. Gogotov IN. Relationships in hydrogen metabolism between hydrogenase and nitrogenase in phototropic bacteria. *Biochimie*. 1978;68:181-186.

2. Rao KK, Hall DO. Hydrogen production by cyanobacteria: potential, problems and prospects. *J. Mar. Biotechnol.* 1996;4:10-15.

3. Tsygankov AA, Borodin VB, Rao KK, Hall DO. H_2 photoproduction by batch culture of *Anabaena variabilis* ATCC 29413 and its mutant PK84 in a Photobioreactor. *Biotech Bioeng.* 1999;64:709-715.

4. Boichenko VA, Hoffmann P. Photosynthetic hydrogen-production in prokaryotes and eukaryotes: occurrence, mechanism, and functions. *Photosynthetica*. 1994;30:527-552.

5. Greenbaum E, Guillard RRL, Sunda WG. Hydrogen and oxygen photoproduction by marine-algae. *Photochem Photobiol.* 1983;37:649-655.

6. Ghirardi ML, Togsaki RK, Seibert M. Oxygen Sensitivity of Algal H_2-Production. *Appl. Biochem. Biotechnol.* 1997; 63-65: 141-151.

7. Melis A, Zhang L, Forestier M, Ghirardi ML, Seibert M. Sustained Photobiological Hydrogen Gas Production upon Reversible Inactivation of Oxygen Evolution in the Green alga *Chlamydomonas reinhardtii*. *Plant Physiol.* 2000; 122: 127-135.

8. Ghirardi ML, Zhang L, Lee JW, Flynn T, Seibert M, Greenbaum E, Melis A. Microalgae: A Green Source of Renewable H_2. *Trends in Biotechnol.* 2000; 18:506-511.

9. Ghirardi ML, Kosourov S, Tsygankov A, Seibert M. Two-phase Photobiological Algal H_2-Production System. In: Proc. 2000 U.S. DOE Hydrogen Program Review, NREL/CP-570-28890 2000.

10. Ghirardi ML, Kosourov S, Seibert M. Cyclic Photobiological Algal H_2-Production. In: Proc. 2001 U.S. DOE Hydrogen Program Review, NREL/CP-610-30535. 2001.

11. Benemann JR. Hydrogen Production by Microalgae. J. Appl. Phycol 2000;12: 291-300.

12. Melis A, Neidhardt J, Benemann JR. *Dunaliella salina* (Chlorophyta) with Small Chlrophyll Antenna Sizes Exhibit Higher Photosynthesis Productivities and Photon Use Efficiencies than Normally Pigmented Cells. *J. Appl. Phycol.* 1999;10: 515-525.

13. Kosourov S, Tsygankov A, Seibert M, Ghirardi ML. Sustained Hydrogen Photoproduction by Chlamydomonas reinhardtii: Effects of Culture Parameters. *Appl. Biochem. Biotechnol*. 2002; 78: 731-741.

14. Harris, EH. The Chlamydomonas Sourcebook. A Comprehensive Guide to Biology and Laboratory Use. San Diego, CA: Academic Press Inc., 1989.

15. Box GEP, Hunter WG, Hunter JS. Statistics for Experimenters. New York: John Wiley & Sons, 1978.

16. Laurinavichene TV, Fedorov AS, Ghirardi ML, Seibert M, Tsygankov AA. Demonstration of sustained hydrogen photoproduction by immobilized, sulfur-deprived Chlamydomonas reinhardtii cells. *Int. J. Hydrogen Energy*. 2006, 31:659-667.

17. Hahn JJ, Ghirardi ML, Jacoby WA. Effect of process variables on photosynthetic algal hydrogen production. *Biotechnol. Prog.* 2004, 20:989-991

4 IMMOBILIZED ALGAL CELLS

4.1 INTRODUCTION

Hydrogen production using photosynthetic green algae is an alternative method for producing hydrogen gas (H_2) as a renewable energy source. Recent work has focused on processes involving *Chlamydomonas reinhardtii*. All reported data to date show hydrogen production far below practical levels as well as cumbersome processing techniques. Therefore, advances in both fundamental microbiology and bioprocess engineering are required for process viability.

One of the main components of the photosynthetic reaction to produce hydrogen is the reversible hydrogenase enzyme, which reduces protons to form hydrogen. Because hydrogenase is so sensitive to oxygen, this reaction must be carried out in an anaerobic environment. Purging oxygen from a reactor system is expensive and impractical from a production point of view.

4.1.1 Background

Melis *et al*. [1] and Ghirardi *et al*. [2] proposed a mechanism to partially inactivate PS II activity to a point where all the oxygen gas (O_2) evolved by photosynthesis is immediately taken up by the respiratory activity of the culture. This mechanism is based on a two-step process. The steps, growth mode and hydrogen

production mode, are initiated by cycling between sulfur-containing and sulfur-free culture medium. This results in a temporal separation of net O_2- and H_2-evolution activities in the green alga *Chlamydomonas reinhardtii*. This discovery eliminates the need for a purge gas, but introduces the need for careful sulfate controls in the aqueous medium.

We have previously studied novel reactor systems and investigated the effects of process variables, including light intensity and transport, cell concentration and mixing as well as reactor design parameters [3]. The potential of using immobilized cells or support structures has also been explored for photosynthetic bacteria [4-6]. Work by Miyake [4] and Tsygankov [5,6] showed that immobilizing cells in a polymeric or glass matrix increases stability and hydrogen yield. Singh [7] showed that bacterial cells can be suspended in micelles to increase hydrogen production rates of bacterial cells. Many of these reactor systems take advantage of the suspended cells to flow fresh medium or purge gases to increase hydrogen yields. However, many of these matrixes utilize expensive materials or have intricate shapes. Low hydrogen yields in all studies to date highlight the importance of breeding better oxygen-tolerant cultures of algae, but the success of photosynthetic hydrogen production also will require progress in process and reactor design.

4.1.2 Objectives

In this chapter, the use of immobilized algal cells to aide in the processing of photosynthetic hydrogen production was investigated. Using the two-step process referenced above requires cycling between a cell growth phase and a hydrogen

production phase. The algal cells must change from a sulfate rich environment to a sulfate free environment by changing the medium in the reaction vessel. Algae immobilized on particle supports can be removed from liquid nutrient solution via filtration. Therefore, expensive and tedious steps such as centrifugation or other techniques are eliminated. The use of particles as support for the algal cells also has an advantage over other systems using solid support because the particles are readily available and inexpensive. This design also has the advantage of easily incorporating into existing or future reactor designs with little or no modification.

4.2 INITIAL IMMOBILIZATION EXPERIMENTS

4.2.1 Growth

Cultures of *Chlamydomonas reinhardtii* were obtained from the National Renewable Energy Laboratory (NREL) on agar plates. Two materials were investigated for use as a solid support. In the initial experiment, we used uniform glass beads. Their lack of buoyancy and low surface area made them unsuccessful candidates. The glass beads remained on the bottom of the flask during agitation. They rubbed together and sheared off any algae growing on them. Visual inspection was sufficient to determine that the algal cells were not adhering to the glass beads and no further testing was done.

The second solid phase tested was fumed silica particles, CAB-O-SIL M-5 (Cabot, Tuscola, IL), with a surface area of 200 m^2/g. Techniques described in Kosourov *et al*. [9] were adapted to grow the algal cultures onto the solid phase. The sulfur-

containing growth medium (TAP+S) was prepared with the addition of a certain quantity of solid phase in the range of 0.1-10 g per liter of growth medium. The new suspension was autoclaved to remove any bacterial contamination before it was inoculated with the algal sample.

As the algal cells were growing on the solid particles, two methods of agitation method were compared. The first method was constant agitation with a magnetic stir bar during the growth phase. The second method involved 1 minute of agitation every 6-8 hours. In between, the solid particles settled to the bottom of the flask. This was done to determine whether intermittent stirring allows algal cells to more readily anchor onto solid particles.

Cell concentration was determined indirectly by measuring chlorophyll concentration [10]. The chlorophyll was extracted by an ethanol solution in this procedure and the residual cell material and solid support was centrifuged off. Assaying chlorophyll concentration spectroscopically, allowed for calculations of a cell concentration for the algal slurry.

The extent of growth is shown in the first row of Table 4.1. There was not much difference between the control case (no silica in the suspension) and the constantly agitated and intermittently agitated suspensions containing silica. The presence of silica did not impede the growth of algal cell cultures.

Table 4.1- Comparison growth, binding and hydrogen production of bound and unbound algal cells.

	Constant Stirring	Intermittent Stirring	Unbound Algae
Avg. Algal Conc. (g ChL/L)	0.0267	0.0231	0.0300
% filtered	97.5%	92.0%	6.5%
H_2 Production (ml H_2/ml susp)	0.209	0.205	0.199

4.2.2 Binding

The extent of how well the algal cells adhered to the solid particles was determined by filtering. A 100 ml sample of algal-solid suspension was passed through a Buchner funnel under pressure with the #1 coarse filter paper under sterile conditions. Three 100 ml aliquots of TAP-S buffer were then passed through the filter to wash any "unbound" algal cells and simulate sulfate removal. The cell density was measured before and after the suspension was passed through the filter to see what percentage of cells was trapped by the filter. Controls were run with unsupported algal cells and silica only suspension.

The second row in Table 4.1 shows the results of the filtration experiments. Unbound algal cells readily passed through the filter and only a small percentage of cells were caught in the filter. Cells grown in the presence of silica particles were predominantly trapped in the filter paper. By comparison, an immeasurable percentage of algal cells were lost when the supernatant was decanted after centrifugation. The separation was slightly higher for the constantly stirred suspensions relative to the intermittently stirred suspensions. A 1% silica solution was filtered and no visible silica particles appeared to pass through. These observations indicate that free-floating cells were too small to be trapped by the filter and that the silica particles were too big to pass through the filter. Thus, the efficient separation of cells from medium in the presence of silica particles indicates the cells were binding to the solid substrate.

4.2.3 Loading

The capacity the solid particles to support algal cells was determined by growing algal cells in constantly stirrer TAP+S media with 3 different concentrations of silica particles: 0.05, 0.1, and 1.0 wt%. Figure 4.1 shows the trend in overall concentration of algae (both bound and free-floating) as a function of time. The abscissa of Figure 4.1 is in units of g chlorophyll/l suspension, which corresponds to algal cell concentration. The close overlap of the three curves indicates that the rate of algal cell growth was (roughly) independent of silica particle concentration. This rate was also similar to that observed for the growth of free-floating algae [3]. The observed similarity supports the data reported in Table 4.1, that the presence of silica did not inhibit the growth of the algae. The drop in chlorophyll concentration seen at the tail of each curve was typical; a drop in algal concentration was seen during the end of the normal growth phase.

Figure 4.2 shows the mass loading ratios of algae to silica [(mass chlorophyll)/(mass silica particles)] as a function of time for the three levels of silica. This figure takes into account the separation efficiency, as only bound algae are included in the numerator. As the algal population grew in the presence of a fixed number of silica particles, eventually binding sites became scarce. Further growth led to an increase in the number of free-floating algae, rather than the number of bound algae.

Figure 4.3 provides further insight into this point. It shows the filter retention of the algae (as described above) as a function of loading ratios. At loading ratios below 0.035, the retention varies between 96-99%. As the loading ratio increases above 0.035, the algal cell retention begins to drop suggesting the attachment sites on the silica particles are saturated.

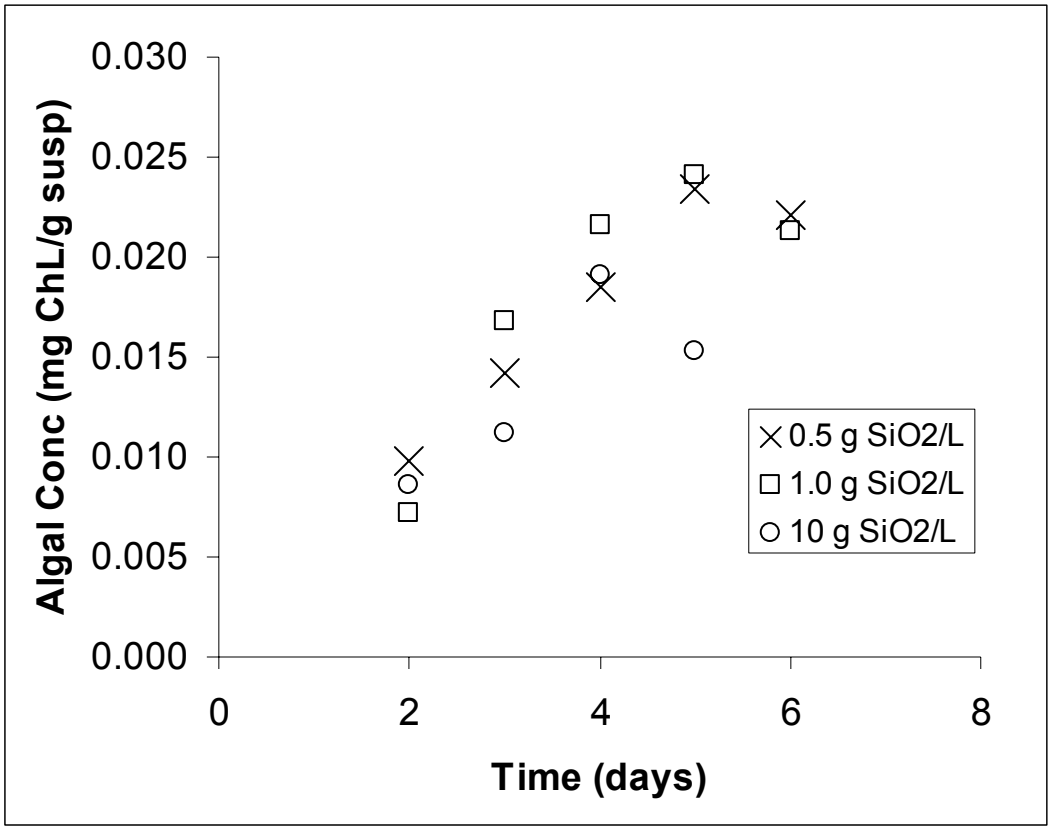

Figure 4.1- Algal concentration measured in g ChL/ml suspension for various silica concentrations.

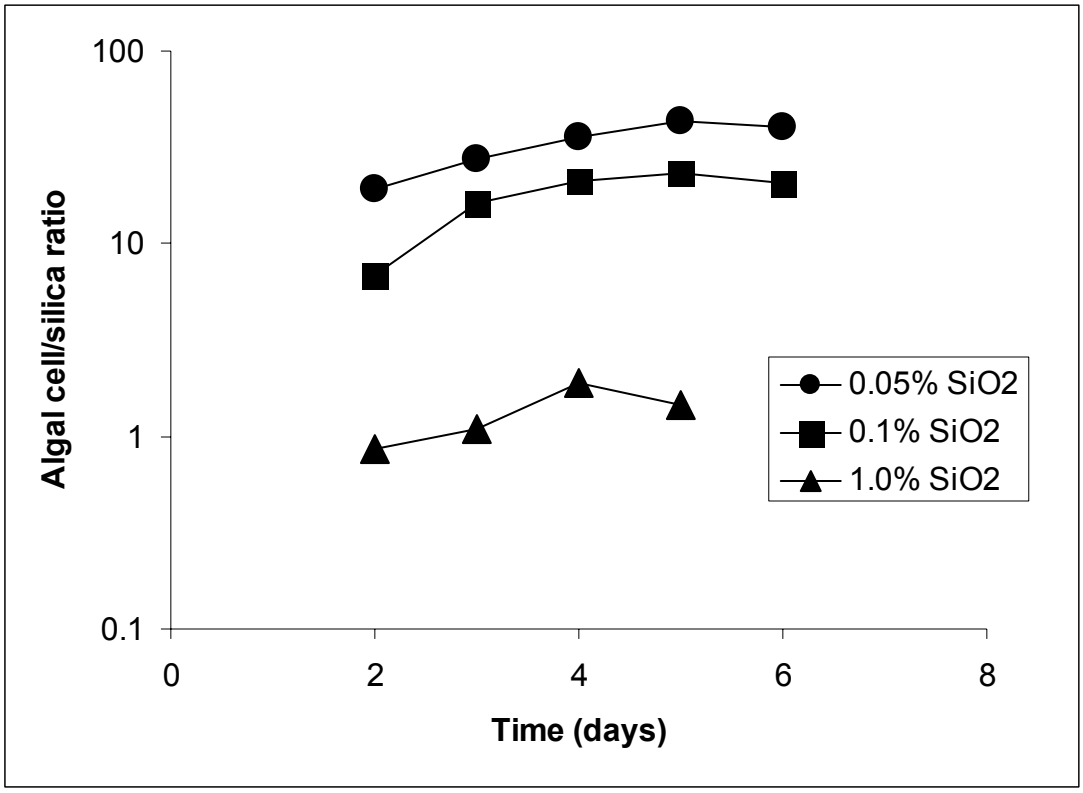

Figure 4.2- The mass loading ratios of algae to silica as a function of time for the three levels of silica.

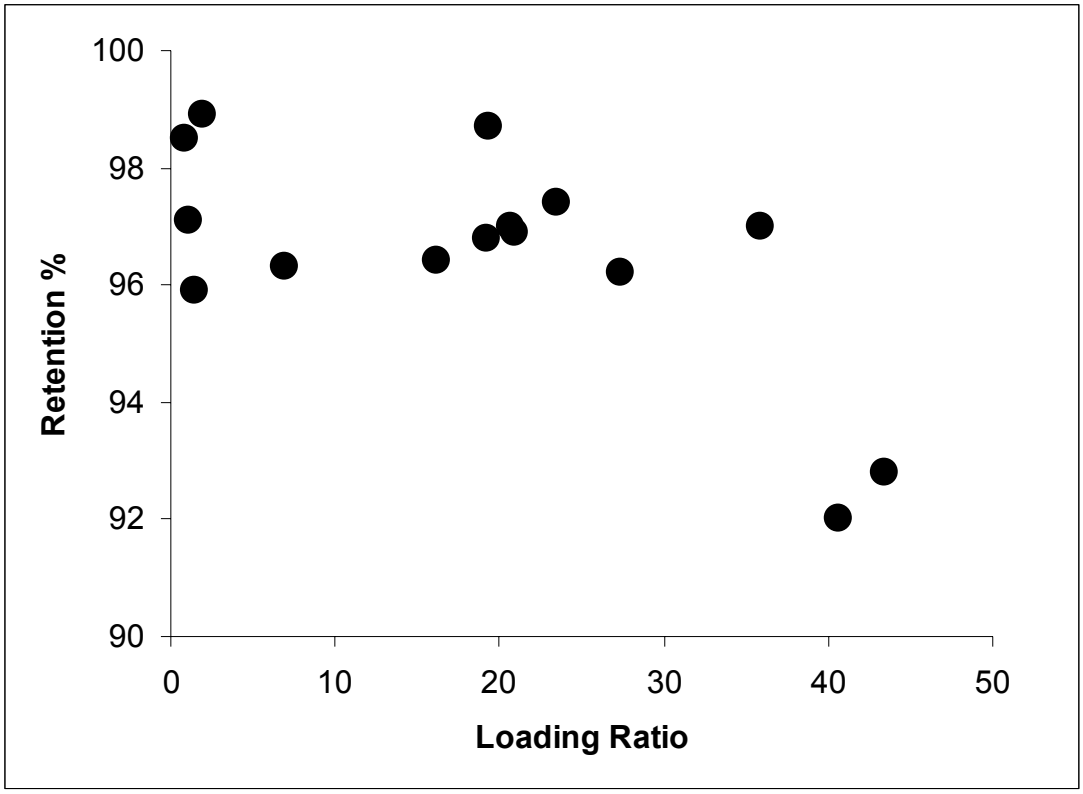

Figure 4.3- Algal cell retention (shown as percentage) for various algal loading ratios.

4.2.4 Hydrogen Production

Results discussed above demonstrate that the algal cells will grow when in suspension with silica particles and that they will bind to the silica particles. It remains to compare the hydrogen production of bound cells to unbound, free-floating cells.

Our previous work [3] showed that hydrogen production was independent of cell concentration between 0.020 and 0.040 g ChL/l. Therefore, the algal cells remained in the growth phase until each suspension's concentration climbed into this interval. After sufficient growth, the cells were removed from the sulfate-containing growth medium via centrifugation. They were suspended in sulfate-free medium and loaded into 250 ml glass Erlenmeyer flask reactors adapted to facilitate and measure hydrogen production [3]. The production phase of experiments was run using 100 $\mu E \cdot m^{-2} \cdot s^{-1}$ light intensity and temperature of 25°C. The concentration of silica in both the constantly stirred and intermittently stirred suspensions of bound algae was 1 wt%.

The third row in Table 4.1 shows that algal cells bound to silica particles produce hydrogen at a very similar rate to free-floating algae.

4.3 SILICA SUPPORTED PERFORMANCE EXPERIMENTS

Chapter 3 discusses the effects on cumulative hydrogen production of several process variables and reactor design parameters [3]. The purpose was to determine the effect of several variables uniquely defined with respect to the bound cell system. These variables were algae concentration (A), silica concentration (S) and the method of

removal of the cells from the medium to cycle between growth and production modes (R). Once again, the response of interest was cumulative hydrogen production (expressed as ml H_2 produced at atmospheric pressure per ml suspension over the entire 96 hour production cycle). A 2^3 full-factorial experiment was performed to assess the sign and magnitude of these effects and their interactions [10].

The variables (factors) and their experimental levels are shown in Table 4.2. Before discussing the results, the execution of the experimental design must be further clarified. Setting both algal concentration and solid phase concentration independently required effort. Algal cells growing in the presence of the specified levels of silica in the TAP+S media were periodically sampled and assayed until the specified cell concentration was achieved. After the growth phase was completed, it was necessary to cycle the cells into hydrogen production mode. This was accomplished in one of two ways and was a categorical variable included in the experimental design (see Table 4.2).

The first method of removing the cells from the TAP+S medium and suspending them in the TAP-S medium used centrifugation and is described elsewhere [3]. The second method of removing the cells from the TAP+S medium utilized filtration. In a sterile environment, the algal cells and solid support were poured through the filter setup, using a vacuum pump to draw out the TAP+S solution. The filtrate was washed 3 times with TAP-S growth medium, through the filter, to remove any excess sulfates. With the vacuum pressure turned off, enough TAP-S media was poured into the filter and stirred around to make a slurry with the cells and solid particles, which was then transferred to another vessel for quantitative suspension and hydrogen production.

Table 4.2- Factor-levels for the full-factorial experiment.

Factor	Low Level (-)	High Level (+)	Units
Algal Conc. (A)	0.015	0.030	g Chl/l
Silica Conc. (S)	1.0	10.	g/ml
Separation Method (R)	Centrifuge	Filtration	

Table 4.3- Factor level assignments during the eight runs of the full-factorial experiment. Also included are cumulative hydrogen production response and the sign and magnitude of the main effects and interactions (M/I).
A= algal concentration, S= silica concentration, R= Sulfate removal technique.

Run	Algal Conc	Silica Conc	Sulfate Removal	A*S	A*R	S*R	A*S*R	H_2 production (ml/ml)
1	-	-	-	+	+	+	-	0.179
2	-	-	+	+	-	-	+	0.185
3	-	+	-	-	+	-	+	0.19
4	-	+	+	-	-	+	-	0.203
5	+	-	-	-	-	+	+	0.261
6	+	-	+	-	+	-	-	0.278
7	+	+	-	+	-	-	-	0.283
8	+	+	+	+	+	+	+	0.272
M/I	0.08425	0.01125	0.00625	-0.0033	-0.0032	-0.0052	-0.0087	

Table 4.3 shows the results of the full-factorial experiment. The effect of going from 0.015 g ChL/l suspension to 0.030 g ChL/l suspension was to increase the cumulative hydrogen production by about 0.08 ml/ml. This is in agreement with our previous work with unbound algae [3]. It should be noted that in that work, we saw a drop off in hydrogen productions at algal concentrations above 0.040 g ChL/l. Laurinavichene *et al*. show higher loading of supported algal cells, beyond that of unsupported cells, can increase hydrogen output [5].

The other main effects and all of the interactions are nearly an order of magnitude smaller in scale. They are all comparable with the magnitude of the three-way interaction, which can be taken as an estimate of the noise in this type of experimental design [10]. Therefore, the effect on hydrogen production of going from 0.001 g/ml to 0.01 g/ml in silica concentration is not significant. This confirms and complements the findings described above; the presence of silica does not adversely effect hydrogen production.

Likewise, the effect of going from the centrifuge-based method to the filtration-based method of cycling between growth and production modes was also not significant. Therefore, the less complex and expensive filtration method can be adopted when using bound algae.

4.4 CONCLUSIONS

Hydrogen production using the photosynthetic algae, *C. reinhardtii*, requires a two-step process. Bound cells are more easily cycled between growth mode and hydrogen production mode. Results presented here indicate that fumed silica is an appropriate solid support for the cells. Neither growth nor hydrogen production is inhibited by the presence of the silica, and the cells are shown to bind to the particles. The silica particles appear to approach saturation algae at a mass loading ratio about 0.035. Increasing the algal cell concentration had a significantly positive effect on cumulative hydrogen production, and higher concentrations should be explored in the context of the bound cell system. Like other reactor systems using solid supported algal cells, silica supported cells can be incorporated to take advantage of features such as medium flow and purge gases. Unlike other systems, this type of solid support system can easily be incorporated in future advancements in the field of reactor design.

4.5 REFERENCES

1. Melis A, Zhang L, Forestier M, Ghirardi ML, Seibert M. Sustained Photobiological Hydrogen Gas Production upon Reversible Inactivation of Oxygen Evolution in the Green alga *Chlamydomonas reinhardtii*. Plant Physiol 2000; 122: 127-135.

2. Ghirardi ML, Zhang L, Lee JW, Flynn T, Seibert M, Greenbaum E, Melis A. Microalgae: A Green Source of Renewable H_2. *Trends in Biotechnol.* 2000; 18:506-511.

3. Hahn JJ, Ghirardi ML, Jacoby WA. The Effect of Process Variables on Photosynthetic Algal Hydrogen Production. *Biotechnol. Prog*. 2004; 20: 989-991.

4. Miyake J, Mao XY, Kawamura S. Hydrogen Production using an immobilized co-culture of anaerobic and photosynthetic bacteria. Proceedings of the International Smposium on Hydrogen Systems. 1985; 1: 277-281.

5. Tsygankov AA, Hirata Y, Miyake M, Asada Y, Myake J. Photobioreactor with Photosynthetic Bacteria Immobilized on Porous Glass for Hydrogen Photoproduction. *J. Fermentation and Bioeng*. 1994; 5: 575-578.

6. Tsygankov AA, Fedorov AS, Talipova IV, Laurinavichene TV, Miyake J, Gogotov IN. *Appl. Biochem. Microbiol.* 1998; 34: 362-366.

7. Singh A, Pandey KD, Dubey RS. Reverse Micelles: a novel tool for H_2 production. *World Journal Of Microbiology & Biotechnology.* 1999; 15: 243-247.

8. Kosourov S, Tsygankov A, Seibert M, Ghirardi ML. Sustained Hydrogen Photoproduction by Chlamydomonas reinhardtii: Effects of Culture Parameters. *Appl. Biochem. Biotechnol*. 2002; 78: 731-741.

9. Harris, EH. The Chlamydomonas Sourcebook. A Comprehensive Guide to Biology and Laboratory Use. San Diego, CA: Academic Press Inc., 1989.

10. Box GEP, Hunter WG, Hunter JS. Statistics for Experimenters. New York: John Wiley & Sons, 1978.

5 THERMOCHEMICAL CONVERSION OF BIOMASS

5.1 INRODUCTION

According to the DOE and USDA, the United States has a supply of 1.3 billion dry tons per year of biomass potential- enough to supply approximately 30% of our current petroleum consumption [1]. Biomass has the potential to be one of the best options for providing a renewable fuel that can be utilized in a range of energy conversion technologies and also has the added advantage of being CO_2 neutral. Supercritical water gasification of biomass has shown great potential for the thermochemical conversion of biomass to produce high concentrations of hydrogen and other gases [2,3]. Unlike conventional pyrolysis and gasification methods, supercritical water can gasify biomass without the expensive and energy-intensive step of drying the feedstock [4].

5.2 BIOMASS

5.2.1 Energy from Biomass

Biomass feedstock encompasses a broad definition of plant and plant derived materials in addition to animal waste products. Biomass currently provides over 3% of

the nation's energy consumption, making biomass based fuels the largest source of domestic renewable energy, surpassing hydropower [1]. In addition to being CO_2 neutral, utilization of fuels derived from biomass can lead to growth in the agricultural sector, reduce imports of oil, and spur new industrial development.

Historically, energy was derived from biomass by direct consumption (*i.e.,* combustion of firewood). Today much of the energy derived from biomass is still utilized through direct means such as industrial heat and steam production by the pulp and paper industry [1]. Energy can also be harnessed from biomass through conversion to more useful forms. Examples include the production of bio-diesel and ethanol as well as thermochemical conversion such as supercritical water gasification of biomass to either liquid or gaseous fuels.

5.2.2 Biomass Structure

Biomass is composed of cellulose, hemicellulose, and lignins. The concentrations of each component vary depending on the feedstock, making assessment of the gasification reaction difficult. Additionally, the structures of hemicellulose and lignins are very complicated, which contributes to the complexity of the thermochemical conversion reactions. Figure 5.1 shows representative structures of each component of biomass.

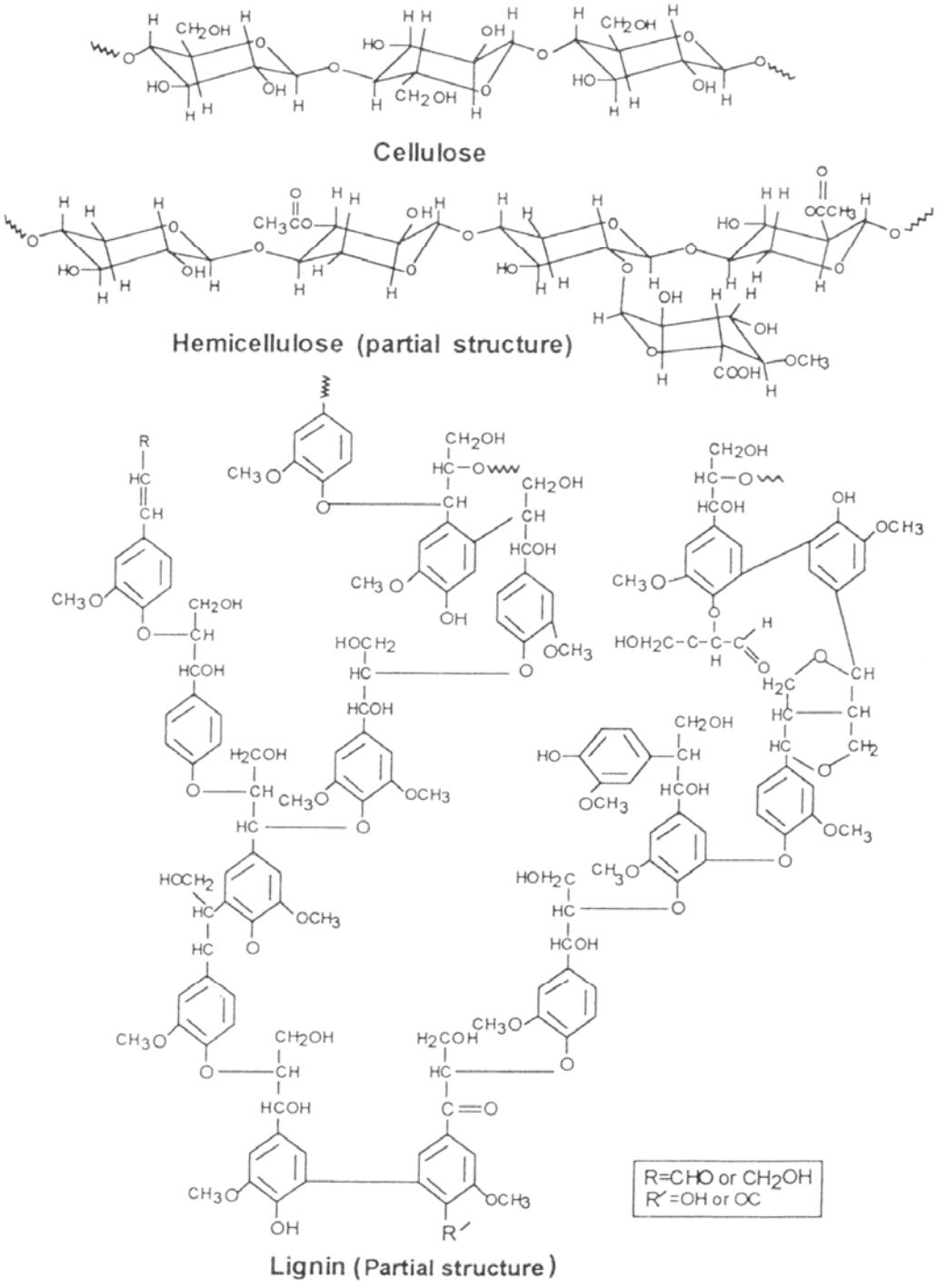

Figure 5.1- Representative polymeric components of biomass [5].

5.2.3 Research Approach

To understand the complex nature of biomass gasification reactions, model compounds, which represent basic structures found within the biomass components, must first be studied. Glucose represents the basic building block of the cellulose polymer and was the focus of this research. Once the glucose conversion is understood, more feeds representing higher degrees of polymerization will need to be studied.

5.3 CONVENTIONAL THERMOCHEMICAL CONVERSION

5.3.1 Pyrolysis

Pyrolysis can be defined as the direct thermal conversion or decomposition of the organic components in the absence of oxygen [6]. In the context of biomass, pyrolysis commonly refers to a lower temperature thermal process producing liquids as the primary product. In addition to liquid fuels, pyrolysis can also yield gasses, charcoal, and useful chemical and food products. Traditional slow pyrolysis has been used to produce charcoal for many years. Fast or flash pyrolysis uses a moderate temperature and much shorter residence time to obtain liquid yields up to 70% and char yields below 5% [7]. However both slow and fast pyrolysis processes require drying- adding considerable expense to the overall process.

5.3.2 Air Gasification

Biomass gasification is designed to produce low- to medium-energy fuel gases, synthesis gases, or hydrogen [6]. In a broader context, gasification can refer to pyrolysis, partial oxidation, or reforming. In this section, only air gasification or partial oxidation is discussed. The first known application of gasification was with coal in 17th century England. Using a less than stoichiometric amount of oxygen required for full combustion, "coal gas" was produced, which was easily transportable and used for heating and lighting [8]. The product yields can be adjusted by varying the temperature and oxygen stoichiometries. However, like pyrolysis, partial oxidation requires the removal of water.

5.3.3 Steam Reforming

Biomass steam reforming mimics conventional methane steam reforming to yield hydrogen gas. In an ideal case, cellulose (represented as $C_6H_{10}O_5$) reacts with steam to produce [9]:

$$C_6H_{10}O_5 + 7H_2O \rightarrow 6CO_2 + 12H_2 \qquad \text{Eq. 5.1}$$

In practice however, steam reforming of biomass yields significant amounts of char and tar while the gas phase contains higher hydrocarbons instead of the desired light gases [9,10]. This is mostly due to biomass not directly reacting with steam to produce the desired products [9]. In the case of steam reforming, the biomass feedstock does not have to be dried, unlike pyrolysis and gasification. However, when water content of the

feed exceeds 40% (as most biomass does), a drastic reduction in the thermal efficiency of steam reforming gasification is observed [4].

5.4 SUPERCRITICAL WATER GASIFICATION

5.4.1 Supercritical Water Properties

Water has a relatively high critical temperature of 374 ºC (647K) and critical pressure of 3200 psia (22.1 MPa). Beyond the critical point, water becomes a fluid with unique properties between those of gas and liquid phases [11]. Supercritical water (SCW) has low viscosity, high diffusivity, and low density compared to liquid water. The dielectric constant is greatly reduced making SCW essentially a non-polar solvent able to solvate organic compounds. The ionic product and dielectric constant of water below its critical point are the major factors controlling hydrolysis reactions of organic materials [12]. Non-polar and slightly polar gases also become soluble in SCW, producing a single fluid phase and minimizing any interphase mass-transport limitations.

Supercritical water gasification of biomass produces high conversion rates of hydrogen and carbon dioxide in addition to carbon monoxide and C1-C4 hydrocarbons [2-4,9]. The properties of SCW are well suited for thermochemical conversion to hydrogen. Compared to steam reforming, SCW offers a homogeneous medium due to its ability to solvate the organic components of biomass. The homogeneous environment lessens the impact of resistance caused by transport phenomena in the heterogeneous environment of steam reforming. The high temperatures and pressures of the process

ensure that intrinsic reaction rates are high [13]. Hydrogen produced under SCW conditions is pressurized which results in smaller reaction and storage container volumes.

5.4.2 Biomass Gasification

The conversion of raw biomass to hydrogen gas consists of a series of complex reactions including pyrolysis, hydrolysis, steam reforming, water-gas shift, methanation, and other reactions [14]. Despite the higher reactivity of SCW compared to steam, not all of the organic materials in biomass are converted to H_2 or CO_2 as evidenced by the formation of chars and tars [3,4,9,10].

Because of the complexity of the biomass reactions, some researchers have taken the approach of studying individual components of biomass. Minowa *et al.* studied the gasification of cellulose and reported hydrolysis is responsible for the decomposition of cellulose, but only in the first stage of conversion [15]. To better understand how the monomeric species of these biomass components react, many other researchers study the SCW gasification of model compounds which correspond to their representative component. Yoshida and Matsumura [16] investigated the supercritical water gasification of xylan as a model for hemicellulose. Hao et al. [13] investigated the supercritical water gasification of glucose as a model for cellulose. Schmieder et al. [4] examined the supercritical water gasification of glucose, catechol and vanillin, and glycine as representative model biomass compounds for cellulose, lignin, and proteins, respectively.

5.4.3 Glucose Gasification

5.4.3.1 Summary

Mok *et al.* reported hemicellulose from various woody and herbaceous biomass samples could be solublized with hot compressed water (34.5 MPa and 200-230 ºC), of which 90% was recovered as sugars [17]. As a result, many researchers have used glucose as a model compound to represent a basic component of biomass. Michael Antal's group at the Hawaii National Energy Institute has done extensive work in the field of biomass gasification including work with SCW conversion of glucose to hydrogen [3,9,14,17,18]. Yu *et al.* reported complete gasification of 0.1 M (*ca.* 1.6 wt%) glucose at 600 ºC and 34.5 MPa but reported lower gasification efficiencies at higher concentrations [14]. Work reported by Xu *et al.* showed they could gasify 1.0 M glucose 98% using activated carbon catalyst at 600 ºC and 34.5 MPa [18]. They also report a significant drop in gasification efficiency when the temperature was lowered from 600 to 500ºC. Sato *et al.* [19] reported that the water-gas shift reaction was very slow at temperatures below 600 ºC, so it is possible the water-gas shift reaction plays a significant role at higher temperatures. Lee *et al.* recently reported completely gasifying 0.6 M (*ca.* 10 wt%) glucose solutions without catalyst at 700 ºC and 26 MPa [20]. There appears to be no recent literature showing higher glucose concentrations completely gasified.

5.4.3.2 Reactor Types

Due to the fibrous or pulpy nature of biomass, many SCW gasification experiments must be done in a batch reactor. Batch reactors have an inherent

disadvantage in that there is less control, especially in terms of heating rate. Even though glucose dissolves to make a homogeneous and easily pumpable solution, problems with char and tar formation make the use of continuous reactors very difficult due to blockage. Some of the recent work with soluble model compounds are still done using a batch reactor [15,16,21,22]. Almost all of the recent work using continuous reactors for glucose SCW gasification use a design based on the system designed by Antal [18] as seen in Figure 5.2. Most designs consists of a high pressure pump which feeds the substrate solution into a tubular reactor inside a furnace. The pressure is controlled by a back pressure regulator. Variations exists, such as additional temperature controls or recycle loops, but the basic premise is a single pump feeding the substrate into the heated zone of the reactor.

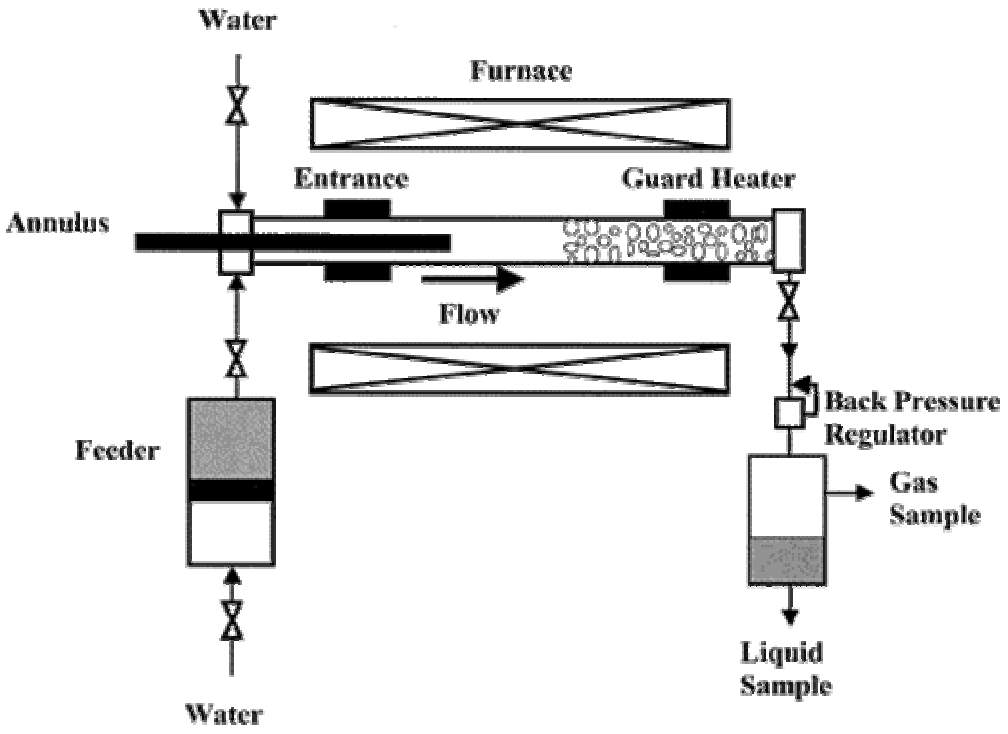

Figure 5.2- Example of a continuous SCW reactor to gasify glucose solutions [3].

5.5 SUMMARY

Biomass has the potential to provide a renewable source of energy. Supercritical water gasification offers a method to convert biomass into usable energy with several advantages over conventional pyrolysis and steam reforming. While much work has been accomplished in glucose gasification, more work needs to be done to overcome the 10 wt% glucose concentration limitation. Overcoming this limit will better ensure a more economical process and prevent blockage in continuous reactor operations.

5.6 REFERENCES

1. Perlack RD, Wright LT, Turhollow AF, Graham RL, Stokes BJ, Erbach DC. Biomass as feedstock for a bioenergy and bioproducts industry: The technical feasibility of a billion-ton annual supply. DOE/GO-102995-2135. 2005.

2. Williams PT and Onwudili J. Composition of Products from the Supercritical Water Gasification of Glucose: A Model Biomass Compound. *Ind. Eng. Chem. Res.* 2005**,** 44:8739-8749.

3. Matsumura Y, Minowa T, Potic B, Kersten SRA, Prins W, van Swaaij WPM, van de Beld B, Elliott DC, Neuenschwander GG, Kruse A, Antal MJ. Biomass Gasification in Near- and Supercritical Water: Status and Prospects. *Biomass Bioenergy* 2005, 29:269.

4. Schmieder H, Abeln J, Boukis N, Dinjus E, Kruse, A, Kluth M, Petrich G, Sadri E, Schacht M. Hydrothermal Gasification of Biomass and Organic Wastes. *J. Supercrit. Fluids* . 2000, 17:145.

5. Lee S. Alternative Fuels. Washington DC: Taylor & Francis. 1996: p 427.

6. Klass DL. Biomass for Renewable Energy, Fuels, and Chemicals. San Diego: Academic Press. 1998.

7. Bridgewater AV, Bridge SA. Biomass Pyrolysis Liquids Upgrading and Utilization. New York: Elsevier Applied Science. 1991.

8. Higman C, van der Burgt M. Gasification. Amsterdam: Elsevier. 2003.

9. Antal MJ, Allen SG, Schulman D, Xu X, Divillo RJ. Biomass gasification in supercritical water. *Ind. Eng. Chem. Res.* 2000, 39:4040-4053.

10. Herguido J, Corella J, Gonzalez-Saiz J. Steam Gasification of Lignocellulosic Residues in a Fluidized Bed at a Small Pilot Scale. Effect of the Type of Feedstock. *Ind. Eng. Chem. Res.* 1992, 31:1274.

11. Arai Y, Sako T, Takebayashi. Supercritical Fluids: Molecular Interactions, Physical Properties, and New Applications. Berlin, Springer. 2002.

12. Clifford, T. Fundamentals of Supercritical Fluids. Oxford: University Press. 1998.

13. Hao XH, Guo LJ, Mao X, Zhang XM, Chen XJ. Hydrogen Production from Glucose Used as a Model Compound of Biomass Gasified in Supercritical Water. *Int. J. Hydrogen Energy* 2003, 28. 55.

14. Yu D, Aihara M, Antal JM. Hydrogen production by steam reforming glucose in supercritical water. *Energy Fuels*. 1993, 7:574.

15. Minowa T, Zhen F, Ogi T. Cellulose decomposition in hot-compressed water with alkali or nickel catalyst. *J. Supercritical Fluids.* 1998, 13:253.

16. Yoshida T, Matsumura Y. Gasification of Cellulose, Xylan, and Lignin Mixtures in Supercritical Water. *Ind. Eng. Chem. Res.* 2001, 40. 5469-5474.

17. Mok WS-L, Antal MJ. Uncatalyzed Solvolsys of Whole Biomass Hemicellulose by Hot Compressed Liquid Water. *Ind. Eng. Chem. Res.* 1992, 31:1157-1161.

18. Xu X, Matsumura Y, Stenberg J, Antal MJ. Carbon-Catalyzed Gasification of Organic Feedstocks in Supercritical Water. *Ind. Eng. Chem. Res.* 1996, 35:2522.

19. Sato T, Kurosawa S, Smith LR. Water-gas Shift Reaction Kinetics Under Noncatalytic Condition in Supercritical Water. *J. Supercrit. Fluids.* 2004, 29:113-119.

20. Lee IG, Kim MS, Ihm SK. Gasification of Glucose in Supercritical Water. *Ind. Eng. Chem. Res.* 2002, 41:1182-1188.

21. Watanabe M, Inomata H, Arai K. Catalytic Hydrogen Generation From Biomass (Glucose and Cellulose) with ZrO_2 in Supercritical Water. *Biomass and Bioenergy.* 2002, 22:405-410.

22. Sinag A, Kruse A, Rathert J. Influence of the Heating Rate and the Type of Catalyst on the Formation of Key Intermediates and on the Generation of Gases During Hydropyrolysis of Glucose in Supercritical Water in a Batch Reactor. *Ind. Eng. Chem. Res.* 2004, 43:502-508.

6 SUPERCRITICAL WATER GASIFICATION OF GLUCOSE

6.1 INTRODUCTION

The objective of the work presented in this chapter was to design and build supercritical water reactors and to use them to determine the effects of several process variables on glucose gasification. A statistical experimental design facilitated our focus on increasing gasification efficiency and feed concentration. Efficiently gasifying biomass in high concentration at short residence time was the long-term goal of this effort.

6.2 CONTINUOUS REACTOR EXPERIMENTS

6.2.1 Experimental Section

6.2.1.1 Continuous Reactor Apparatus

Figure 6.1 shows the schematic of the supercritical water (SCW) continuous reactor. The reactor was constructed from an 8" length of 316 stainless steel tubing (0.75" OD x 0.438" ID) obtained from High Pressure Equipment (HiP). The reactor and fittings had a pressure rating of 20,000 psi. The reactor system was plumbed using 316

stainless steel tubing (0.25" OD x 0.083" ID) fitted with High Pressure fittings (HiP) rated at 60,000 psi. The organic substrate was fed using a piston pump (Eldex B-100) while the water stream was fed using a smaller piston pump (Eldex A-30S). The water stream passed through a preheating furnace through a coiled 60 inch length of 0.25" tubing. The organic stream and supercritical water stream merged just prior to the main reactor. A 1/16" thermocouple was fitted in a 4-way tee to measure the temperature of the two merging streams. Another thermocouple was attached to the outside wall of the reactor to approximate the temperature of the reaction. The product stream exited the reactor and was chilled in a tube heat exchanger to quench the reaction. The reaction products then passed through a 20 micron filter to trap any large particles. Pressure was controlled using a metering valve (HiP) with a long stem designed to handle high temperatures. The products were then sent through a vapor-liquid separator where the 2 streams were collected and measured.

6.2.1.2 Characterization

Gas samples were characterized using an HP 5890 gas chromatograph (GC) with a Supelco 80/60 Carboxen molecular sieve column (15 ft x 1/8" SS), argon carrier gas and a thermal conductivity detector (TCD). The oven temperature was initially set at 40ºC and the detector was set at 200ºC. The oven temperature was held at 40ºC for 8 min, then ramped to 140ºC at 20 degrees/min and held for 9 minutes. The flow rate of argon was between 6.5 and 8 ml/min, with a column head pressure of 200 KPa and an argon supply pressure of approximately 105 psi. This setup was able to measure small

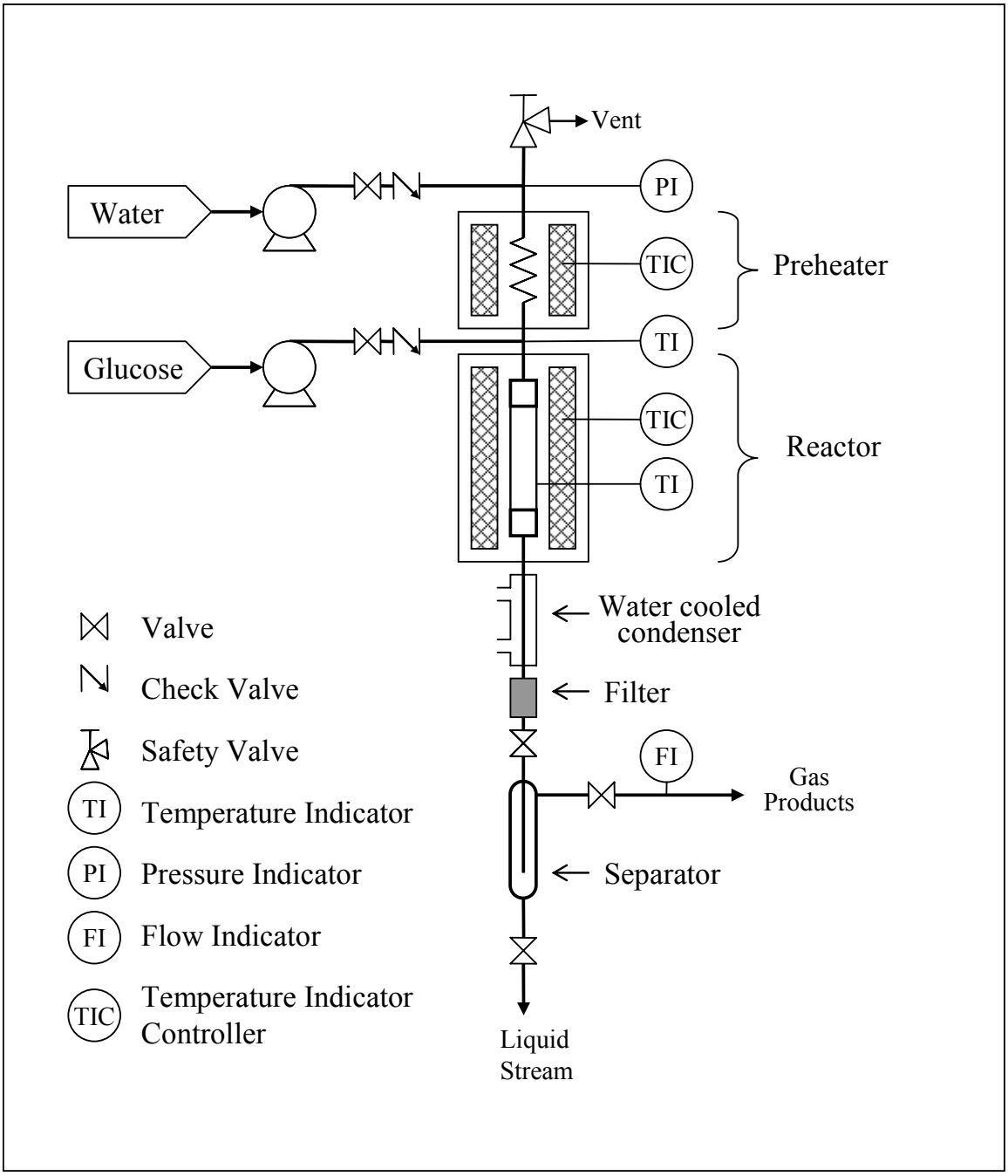

Figure 6.1- Schematic of the supercritical water reactor

molecules up to C-3. The liquid phase was analyzed using a total organic carbon analyzer (TOC). Once a carbon mass balance was established, only GC was used to characterize the gas products since the objective of the work was studying gasification.

6.2.1.3 Continuous Reactor Operation

Anhydrous *D*-glucose was obtained from Sigma. Samples were purged with nitrogen then degassed under vacuum. The distilled water was also prepared in a similar manner. The glucose and water feed were pumped into the reactor in a 2:1 ratio and as a result, the glucose concentration was increased 50% to accommodate the final desired concentration. Without the superheated water stream, the organic stream entered into the mixing tee at a temperature of approximately 250ºC due to heat conducting through the tubing from the furnaces. The superheated water stream entered the mixing tee at a temperature of approximately 800ºC. When the two streams merged, the temperature cycled between 400-430ºC due to the cycling of the piston pumps. The temperature was slightly lower than expected, most likely due to phase change enthalpy, but is still above the critical temperature indicating the mixture is supercritical when it reaches the mixing tee.

The feed rate was determined using the desired residence time and density of the sc-H_2O at the desired pressure and temperature for the given reactor volume. The sc-H_2O density values were obtained from Kirillin *et al.* [1] and Arai *et al.* [2] The effect of glucose was ignored and the solution density was assumed to be that of pure water. Table 6.1 shows the correlation between density, residence time, reactor size, and flow rates.

Table 6.1- Correlation between density, reactor volume and residence time

Temp (C)	Press (psi)	Density (kg/m^3)	Res. Time (sec)	Reactor Vol (ml)	Flow Rate (ml/min)
750	4000	64	40	28.3	2.72
750	5000	80	40	28.3	3.40
600	4000	80	40	28.3	3.40
600	5000	105	40	28.3	4.46
750	4000	64	12	8.5	2.72
750	5000	80	12	8.5	3.40
600	4000	80	12	8.5	3.40
600	5000	105	12	8.5	4.46

Once the furnaces reached the desired temperatures, glucose solution was fed into the reactor. The reactor ran for at least 1 hour to make adjustments to the metering valve to control back pressure and ensure steady state conditions. Rates of the glucose solution and water feed as well as the final liquid product were measured using mass differences for the given time period. Gaseous products rate was measured using a dry test meter.

6.2.1.4 Statistical Design of Experiments

In an effort to learn how to efficiently gasify glucose in high concentrations and a short residence time, a $2^{(5-2)}$ Resolution III partial factorial experimental design was used to evaluate the effect of five variables on several process outputs. The variables (factors) were temperature, pressure, presence or absence of homogeneous catalyst, feed concentration and residence time. These factors and their levels are shown in Table 6.2. As this is a partially saturated Resolution III design, main effects can be confounded with two-way interactions. A partial confounding pattern is shown in Table 6.3.
The feed concentration of 10 and 20% glucose correspond to approximately 0.6 and 1.2 M respectively. 10 and 20% were chosen because 0.6 M or 10% was the highest reported feed concentration that was successfully gasified by Lee *et al.* [3]. Hao *et al.* reported a thick tar like substance in the liquid phase when they attempted to gasify a 0.8 M (*ca.* 15 wt%) glucose solution, indicating incomplete gasification. Because of the limitation of the feed pumps, residence times were adjusted by changing the size of the reactor. Reactor volumes of 8.5 and 28.3 ml corresponded to residence times of 12 and 40 seconds, respectively.

Table 6.2- Effects measured showing low and high levels.

Effect		Low Level	High Level
Temperature	(Temp)	600C	750C
Pressure	(Pres)	4000 psi	5000 psi
Catalyst	(Cat)	None	KOH
Feed Conc	(Conc)	10 wt%	20 wt%
Res Time	(Tau)	12 sec	44 sec

Table 6.3- Confounding rules and aliasing structure for screening factorial

Fractional Factorial Structure **Factor Confounding Rules**	
Temp	Tau*Pres*Conc
Cat	Pres*Conc
Aliasing Structure	
Tau	Temp*Cat
Pres	Conc*Cat
Conc	Pres*Cat
Temp	Tau*Cat
Cat	Tau*Temp or Pres*Conc
Tau*Pres	Conc*Temp
Tau*Conc	Pres*Temp

Please see Table 6.1 for more information on residence times and flow rates. Potasium Hydroxide (KOH) was used as the catalyst for this experiment. The KOH was added to the glucose feed solution at 10% of the glucose concentration. The temperature of the reaction was set by adjusting the main furnace surrounding the reactor. The furnace was set such that the temperature reading of the thermocouple on the outside reactor wall read 50ºC higher than the desired temperature. This was a rough estimate of the difference between the reaction zone and the wall temperature. Pressure was set by adjusting the back pressure metering valve while monitoring the reactor pressure.

The effects of the process variables discussed above were determined for three responses: overall gasification efficiency (GE), carbon efficiency (CE) and H_2 yield. Each response was calculated as a percentage. Gasification efficiencies were calculated by measuring the mass flow rate of the gas evolved divided by mass flow rate of the glucose fed.

$$\mathrm{GE} = \frac{[\mathrm{Gas\,Molar\,Flow\,Rate}] \times [Ave\,MW]}{[\mathrm{Glucose\,Mass\,Flow\,Rate}]} \times 100 \qquad \text{Eq. 6.1}$$

The output gas molar flow rate was calculated from the volumetric gas flow rate, assuming Ideal Gas Law. The average molecular weight of the gas was determined by GC analysis. The gasification efficiency of carbon, hydrogen, and oxygen were determined by dividing the total moles of carbon (hydrogen or oxygen) atoms of each gas in the product stream by the total moles of each carbon (hydrogen or oxygen) atom in the glucose feed.

$$\mathrm{CE} = \frac{[\text{Gas Molar Flow Rate}] \times [1 \cdot x_{CO_2} + 1 \cdot x_{CH_4} + 2 \cdot x_{C_2H_6} + \ldots]}{6 \times [\text{Glucose Molar Flow Rate}]} \times 100 \qquad \text{Eq. 6.2}$$

Hydrogen and oxygen efficiencies were calculated in a similar manner. The H_2 yield was calculated by calculating the number of moles H_2 evolved divided by half the available number of hydrogen atoms available.

$$\mathrm{H_2\,Yield} = \frac{[\text{Gas Molar Flow Rate}] \times [x_{H_2}]}{6 \times [\text{Glucose Molar Flow Rate}]} \times 100 \qquad \text{Eq. 6.3}$$

6.2.2 Results

6.2.2.1 Factorial Results

Table 6.4 shows the results of the factorial experiments and the experimental conditions. The gas products consisted mainly of H_2, CO_2, CH_4, CO, and, to a lesser extent, C_2H_6, C_2H_4, and N_2. The mole fractions of each of the major products are shown. The H_2 yield is also shown in this table.

Table 6.4- Gas Phase and Gasification Efficiencies of Supercritical Water Glucose Gasification.

Run	1	2	3	4	5	6	7	8
Tau	12	12	12	12	40	40	40	40
Pres	4000	4000	5000	5000	4000	4000	5000	5000
Conc	0.1	0.2	0.1	0.2	0.1	0.2	0.1	0.2
Temp	600	750	750	600	750	600	600	750
Cat	Yes	no	no	yes	yes	no	no	yes
				Gas Phase Mole Fractions				
H_2	0.305	0.366	0.439	0.219	0.261	0.169	0.352	0.387
CO	0.473	0.065	0.000	0.059	0.000	0.529	-0.010	0.025
CH_4	0.194	0.163	0.183	0.093	0.322	0.119	0.250	0.205
CO_2	0.014	0.355	0.377	0.615	0.417	0.183	0.409	0.382
C_2H_6	0.014	0.051	0.000	0.014	0.000	0.000	-0.001	0.000
				Gasification Efficiencies and Yield (%)				
Overall	67.7	113.5	108.4	40.9	80.6	41.7	57.2	61.9
C	58	105	89	31	74	41	50	53
H	60	129	129	18	91	20	65	69
O	41	118	120	51	84	45	62	68
H_2 Yield	28.4	55.9	70	8.64	26.3	8.42	27	33.3

Table 6.5 shows the effect of each of the variables on the responses of interest. These numbers may be interpreted as the average change observed in the response(s) when going from the minus level (e.g., Temp = 600ºC) to the plus level (e.g., Temp = 750ºC) for any particular variable. The responses were measured in terms of overall gasification efficiency (GE), carbon gasification efficiency (CE) and H_2 yield. CE and H_2 yield were measured in addition to overall gasification efficiency because the potential water-gas shift reaction may have artificially increased the overall gasification efficiency.

When the responses are plotted on normal probability paper, the only variable that attains statistical significance is temperature. Increasing the temperature from 600ºC to 750ºC led to double-digit percentage increases in all responses (GE, CE & HE). These results are consistent with the work by Lee *et al*. [3], where they report increasing H_2 yields and overall gasification efficiencies with higher temperature. The higher temperature may also favor reactions involving supercritical water as a reactant as well as a solvent. It should be noted that the overall hydrogen and oxygen gasification efficiencies range to a maximum value greater than one (*e.g.*, runs #2 and #3 in Table 6.4). This is an indication that supercritical water is a reactant as well as a solvent in the gasification reaction. One possibility is the water-gas shift reaction, which may be responsible for the low levels of CO observed in these runs.

Table 6.5- Measured Responses of Gasification and H_2 Yield

Effect	Overall Gasification	Carbon Gasification	H_2 Yield
Tau	-11.1	-7.8	-8.5
Pres	-4.4	-6.6	2.5
Conc	-7.0	-4.9	-5.7
Temp	19.6	17.7	14.1
Cat	-8.7	-8.7	-8.1

Normal probability analysis identifies significant variables, but is prone to Type II errors (concluding something is not significant when it is) [5]. The confounding pattern shown in Table 6.3 further muddies the waters. Therefore, further clarification was sought with respect to residence time (tau) and the presence or absence of KOH catalyst. Table 6.5 shows the effect of these variables have the next highest magnitude after temperature. To learn more about the effect of these variables, runs #2 and 8 were replicated with the catalyst variable inverted. The resulting 2x2 matrix compares the effect of residence time and catalyst while keeping temperature and concentration constant at 750ºC and 20% respectively. Pressure was not kept constant but was not shown to have a significant effect in this range. Figure 6.2 shows the results of the revised 2x2 matrix. Residence time did not appear to have a significant effect. Additional time beyond 12 seconds did not appear to benefit yields or gasification efficiencies.

The use of KOH catalysts does appear to negatively affect gasification efficiency and hydrogen yield. Alkali bases have been used in many glucose and biomass supercritical water gasification studies [4,6-9]. However for this glucose case, KOH catalyzes a hydrolysis reaction at sub-critical temperatures which can affect the subsequent supercritical thermochemical conversion to hydrogen and other gasification products. More details concerning the mechanism and pathways are discussed in Section 6.3.2.

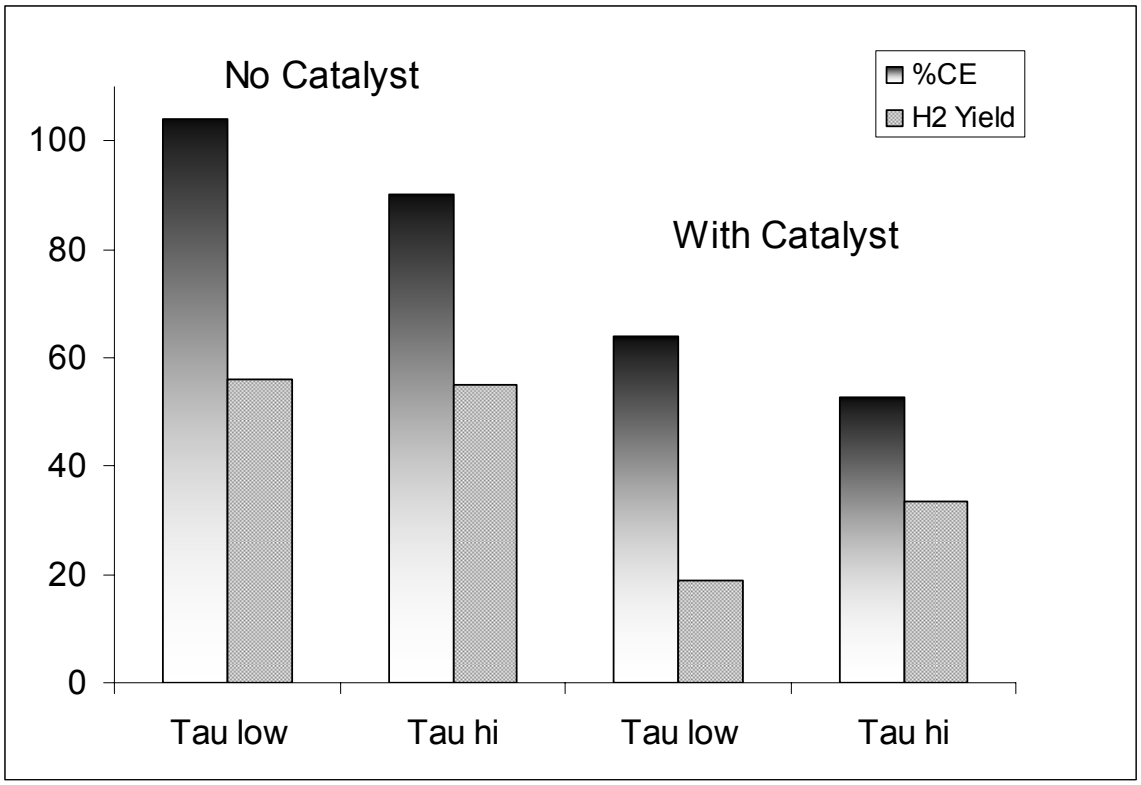

Figure 6.2- 2x2 matrix comparing residence time (tau) and catalyst loading.

Table 6.5 also shows the effect of glucose feed concentration. As concentration increased from 10% to 20% (*ca.* 0.6 M to 1.2 M), no significant effect was observed. Unlike other results [4,10], the reactor setup used in this experiment can accommodate higher feed concentrations without a decrease in gasification efficiency.

The original screening factorial had an additional factor to test- a comparison of mixing the glucose feed with a supercritical stream of water versus a cold stream of water, before entering the hot reactor. The test was designed to mimic continuous reactor designs presented by other authors where the glucose feed was gradually heated as it passed through the furnace as opposed to the current system where the glucose feed was almost instantaneously brought to supercritical conditions. This factor was removed because char accumulated in the mixing tee when using a sub-critical water stream, effectively blocking any flow and preventing any experimental runs. This observation shows mixing the glucose feed with hot supercritical water is critical to complete gasification.

Because changing the feed concentration from 10% to 20% had no significant effect on gasification and H_2 yield, the glucose feed concentration was raised to 30%. Figure 6.3 shows the results of 10, 20, and 30%. The reaction was run at 750C, 5000 psi, 40 second residence time, no catalyst, and the glucose feed to water ratio was 2:1 ratio. Performance dropped significantly at the higher concentration. This reactor setup was not able to gasify the higher concentration of glucose. This observation may be explained by examining the rate at which the substrate was heated up.

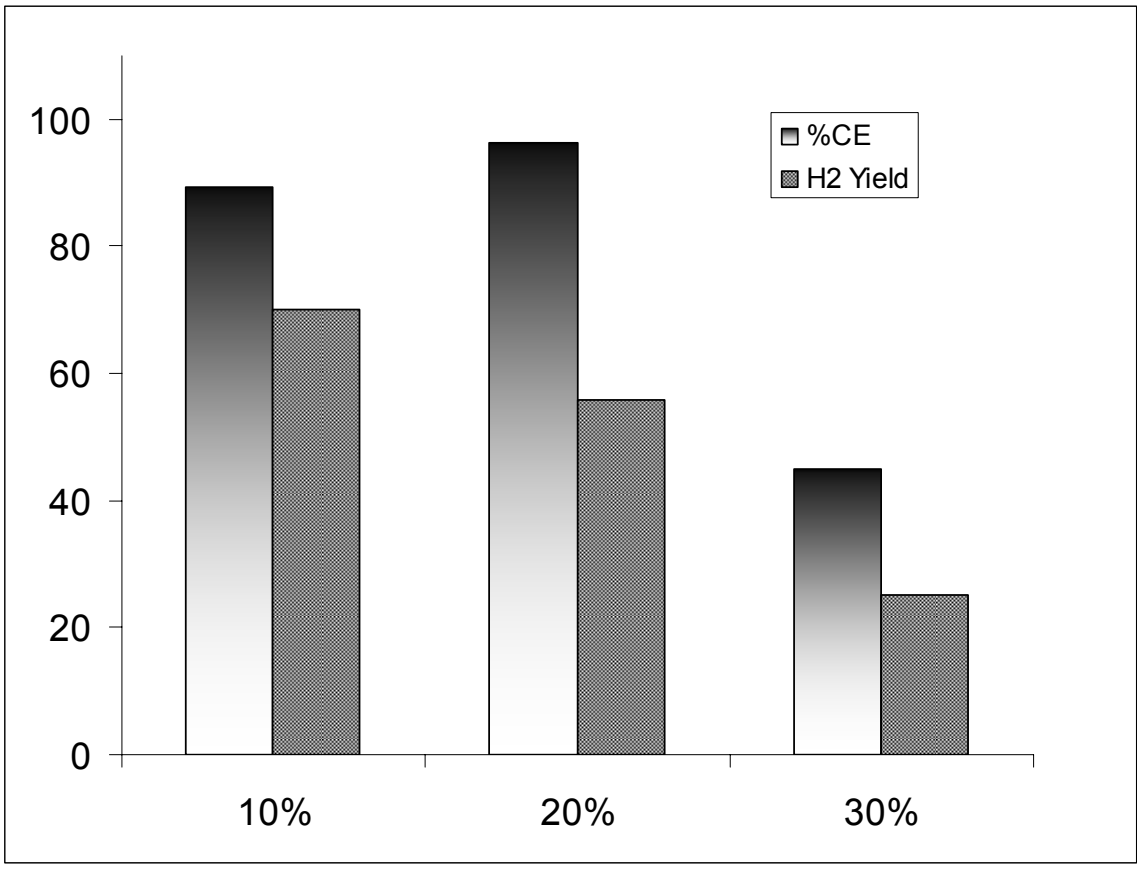

Figure 6.3- Effect of Glucose Feed Concentration on Gasification Efficiency and H_2 Yield.

6.2.3 Lactose Experiments

Lactose was chosen as the next test substrate to undergo supercritical water gasification because it is in a class of sugar compounds known as disaccharides- a dimer of two 6-carbon sugars. A 20 wt% solution of lactose was gasified using the 28.3 ml continuous reactor at 750ºC and 4000 psi. A sample of concentrated milk permeate was obtained from North American Milk Products. The milk permeate is the result of separating fats and proteins from milk and is mostly composed of lactose. The 25% solids permeate had a concentration of 20% lactose as determined by HPLC. Currently, milk permeate is treated as waste and therefore offered a unique opportunity to study a biomass sample found in the dairy industry. The results are shown in Figure 6.4 with 20% glucose results as a comparison.

The gasification efficiencies of glucose and lactose appear to be comparable. These results indicate molecules approximately twice the molecular weight of glucose can be gasified without the use of an oxidant. Also, the aldehyde bond which bonds the two glucose molecules does not appear to have a significant effect on the gasification mechanism. Shafizadeh [11] presented a mechanism for cellulose pyrolysis where cellulose depolymerizes to β-glucosan, which can also form upon the dehydration of glucose. It is premature at this point to suggest a mechanism, but the possibility exists that lactose and more complex polysaccharides may follow a comparable path of glucose gasification if the polysaccharide undergoes depolymerization as the first step.

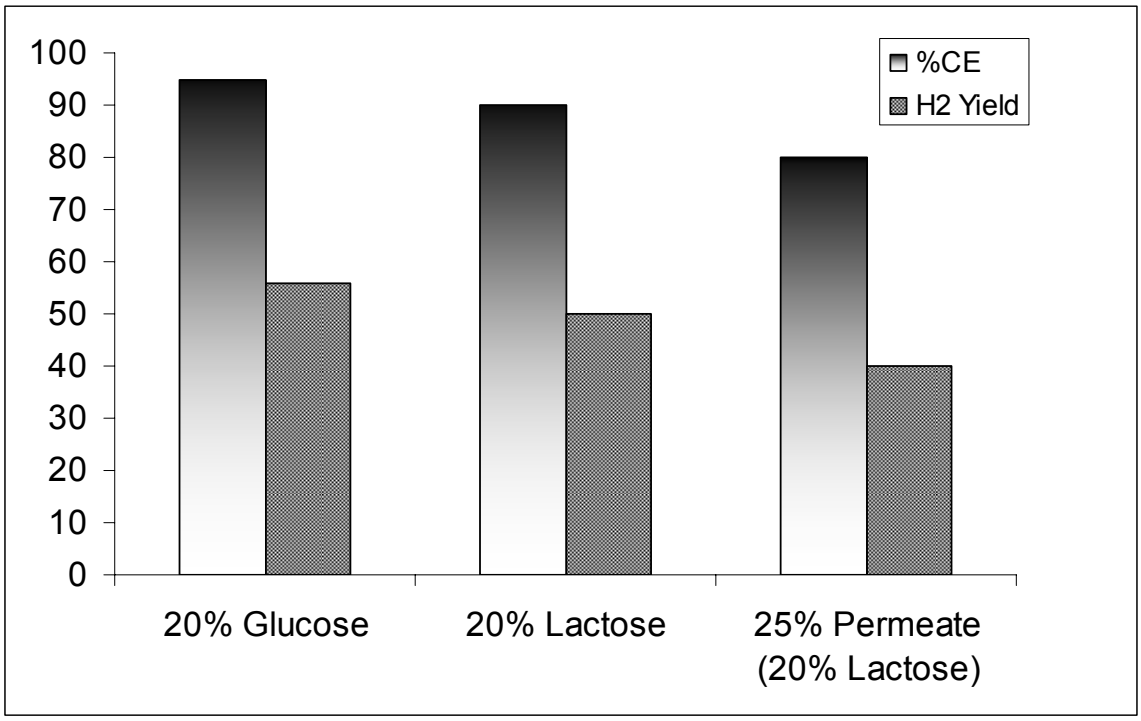

Figure 6.4- Gasification results of 20% Lactose and 25% Milk Permeate (equivalent to 20% Lactose).

The milk permeate results also indicate that it gasifies in a similar manner to lactose. What was not measured in these experiments is the amount of char that was formed by the reaction. In addition to lactose, permeate contains other sugars, small peptides and inorganic matter.

6.3 BATCH REACTOR EXPERIMENTS

6.3.1 Experimental

6.3.1.1 Batch Reactor Apparatus

In an effort to understand mechanisms, particularly the "hot water" chemistry during heat up and cool down, and explore other feed substrates, a batch reactor was built. It was constructed from 316 stainless steel tubing obtained from HiP. The 8" length of 1" OD (9/16" ID) had an internal volume of 50 ml and was threaded with a medium pressure fitting rated at 20,000 psi. Each end was fitted with a 3" cap, also made from 316 stainless steel.

6.3.1.2 Batch Reactor Procedure

In an effort to test other substrates, the HiP micro-reactor was used to gasify solids not capable of being run in the continuous reactor. To correlate the results of the two sets of reactors, conditions similar to Run #2 of Table 6.4 were tested in the batch reactor. Using SCW density data [1,2], a 5 ml solution of 20 wt% glucose was calculated to achieve at least 5000 psi at 750ºC for the given reactor volume and was subsequently

loaded. The batch reactor was buried in a sand bath inside a furnace preheated to 750ºC. The reactor was removed after 30 minutes and allowed to air cool overnight.

6.3.1.3 Gasification Calculations

Overall gasification efficiency was determined gravimetrically. To verify absence of leakage, the mass of the sealed reactor was measured before the reaction and after the batch reactor had cooled to room temperature. Then the reactor was opened, releasing the permanent gas products. The reactor was weighed again to determine the mass of the gas products based on the weight difference. The liquid was carefully poured out of the reactor and the reactor was dried under a nitrogen gas stream. If any solids poured out with the liquid, those products were filtered and dried. The dried reactor was then weighed. The reactor was cleaned, dried and weighed again. The difference in weights, in addition to the solids collected, represented the weight of the char.

In some cases of high gasification efficiencies, enough pressure remained in the reactor after cooling to ambient temperature that liquid was displaced, along with the gas, when the seal was broken. In these cases, chilling the batch reactor in the freezer allowed accurate estimation of the mass of the permanent gases. The pressure was then low enough such that opening the reactor did not result in a violent discharge of gas and liquid. The reactor was then sealed and placed in a 50ºC oven for 1-2 hours to evaporate any condensation on the exterior of the reactor. The reactor was allowed to cool to room temperature, the remaining pressure was released, and the reactor was then weighed.

6.3.2 Results

6.3.2.1 Glucose Gasification

10% and 20% solutions of glucose were gasified using the micro-batch reactor under conditions similar to Runs #2 and #3 from Table 6.4. Gasification efficiencies ranged between 40-50% as opposed to the near 100% gasification efficiencies found in the continuous reactors. The thermal mass of the batch reactor results in significant heat up time in which non-productive chemistry can occur. This is not the case for the continuous reactor, which features near instantaneous heating in the mixing tee.

6.3.2.2 Char Formation

Onwudili *et al*. [12] observed significant char formation when glucose temperature rose above 250ºC. Exploration of hot water chemistry suggested a comparison of the effect of heating rate on the formation of char and the formation of gasification products. To this end, a series of batch reactor experiments was performed to test the hypothesis that char formation occurs primarily at subcritical temperatures.

Figure 6.5 shows the gasification efficiencies and char yields of batch reactor experiments where the temperature was held at 300ºC to insure char production. These results were compared to 20% glucose solutions heated to 300ºC for 30 minutes then heated to 750ºC for another 30 minutes. While the gasification yields increase to 50%, the char yield does not change significantly. Figure 6.5 also shows the results of a batch reaction run at 750ºC in the sand bath.

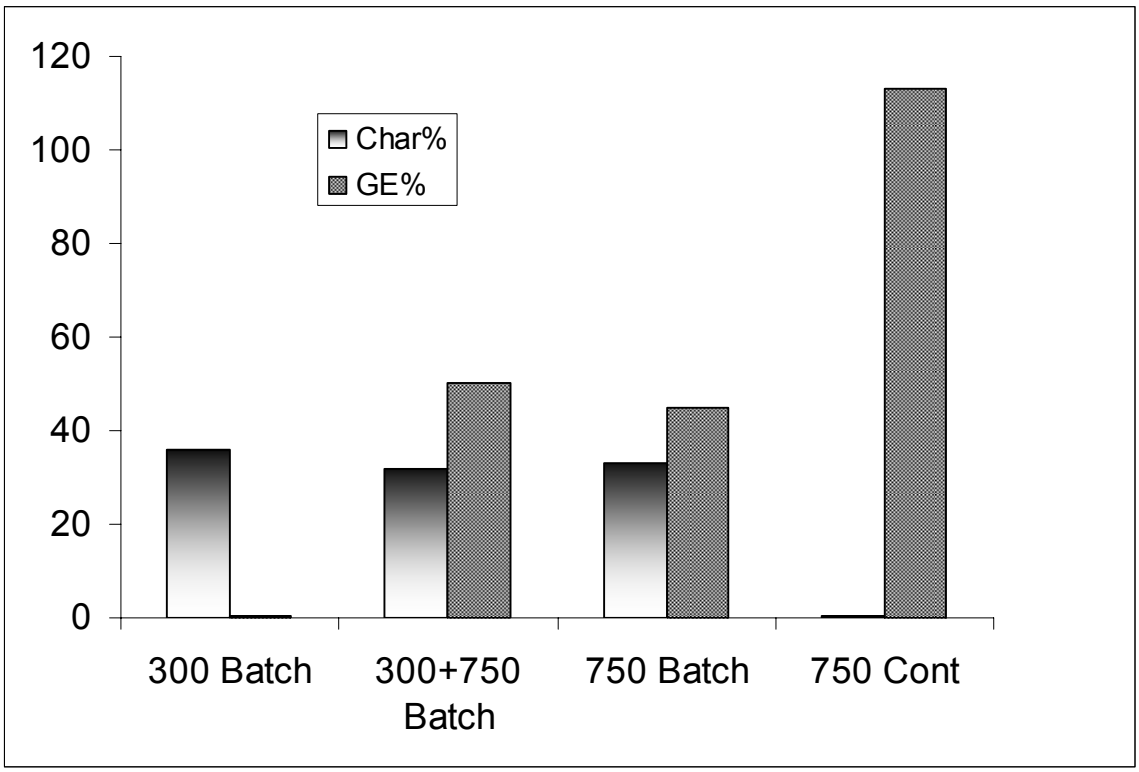

Figure 6.5- Batch reactor experiments comparing gasification efficiencies and char formation of a deliberately slow heating time.

These results reveal the sand bath was not hot enough or did not transfer enough heat fast enough to the batch reactor of this size and mass. The results of the comparable continuous reactor run are also shown in Figure 6.5 and demonstrate a clear advantage over batch reactors. Char formation is minimized when reactants reach supercritical conditions very quickly.

The second conclusion from this data is that once the char is formed, it does not break down into gasification products in an anaerobic supercritical water medium. The liquid decanted from the 300ºC batch reactor experiment was a dark brown liquid. The liquid decanted from the 300+750ºC and 750ºC experiments were both clear. These observations would indicate supercritical water can gasify organic matter which has not solidified, but once the char reaction has proceeded to the solid black phase, supercritical water appears to have no effect. This proposed mechanism is outlined in Figure 6.6. The "hot water" chemistry of hydrolysis appears to be inevitable as indicated by the 30% glucose experiment seen in Figure 6.3. If the extent of hydrolysis is low before the substrate reaches supercritical conditions, it appears supercritical water can gasify the partially hydrolyzed glucose. If the hydrolysis reaction occurs to the point of char formation, sc-water cannot gasify the char without an oxidant or some other mechanism.

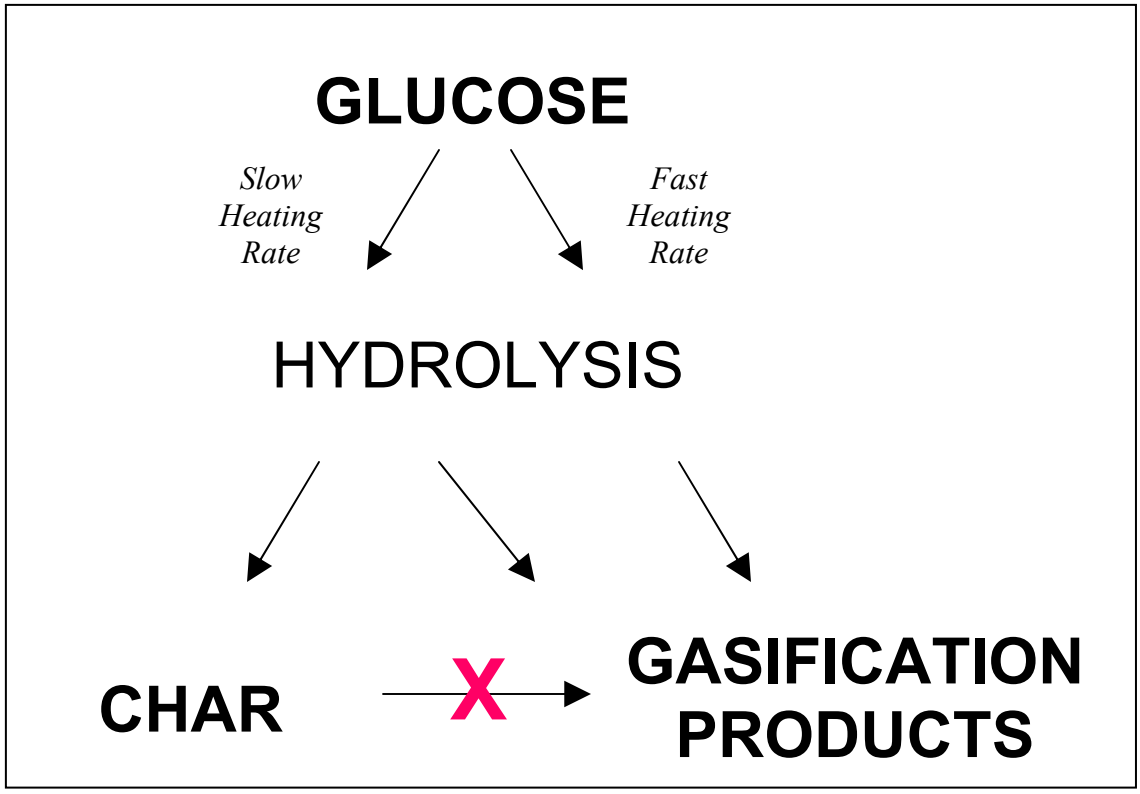

Figure 6.6- Proposed mechanism of glucose gasification. Slower heating rates favor char formation.

6.4 HEAT TRANSFER IN CONTINUOUS REACTORS

Hao *et. al.* [4] observed a decrease in glucose gasification efficiency when they increased the reactor ID from 6 mm to 9 mm in a continuous tubular reactor. The decreased efficiency was more pronounced as they increased the glucose concentration from 0.4 M to 0.8 M. These observations indicated a 2-way interaction takes place between ID and concentration where the combined effect of increasing ID and concentration decreases efficiencies more so than the two individual contributions. The authors attributed this observation to the surface area to volume ratio. Onwudili *et al*. [12] observe significant char formation when glucose temperature rose above 250ºC. In the case of continuous tube reactors, as the glucose feed travels down the tube, the bulk temperature of the solution increases as it approaches supercritical temperatures. Once the temperature reaches 250ºC, a hydrolysis reaction resulting in char occurs.

6.4.1 Conventional Continuous Tube Reactor

The effect of heat transfer can be further explored by examining a simplified model of a tubular reactor as shown in Figure 6.7. As the fluid enters the heated portion of the tubing, the bulk temperature of the fluid rises. Assuming axial conduction, kinetic energy flux and work terms are negligible; the system can be modeled using a shell balance as shown below:

$$Q + wC_pT_1 = wC_pT_2 \qquad \text{Eq. 6.4}$$

Q is the heat flow into the system; w is the fluid flow rate; C_p is the heat capacity; and T_1 and T_2 are bulk temperatures of the fluid at the entrance and exit of the system. Because we are interested in the region where the temperature of the fluid is between 250 and 380ºC, T_1 and T_2 are defined as 250ºC and 380ºC respectively. Each term of Eq 6.4 is assumed to be constant if the only variable to change is the size of the tubing. The heat term Q can be expressed as:

$$Q = h(\pi DL)\Delta T \qquad \text{Eq. 6.5}$$

h is the heat transfer coefficient; ΔT is the temperature difference between the tube wall and bulk temperature of the fluid; and πDL refers to the surface area of the fluid exposed to the tube wall in the differential volume defined by the system in Eq. 6.4. Because the tubing is placed in a furnace set at a constant temperature, ΔT is assumed to be constant. As the tubing diameter increases, the surface area to volume ratio decreases. As a result, the length of tubing as defined in this system must increase to keep the heat term constant. The residence time specific to this temperature range is then increased as the overall system volume increases. If the char reaction is assumed to be anything other than zero-order for glucose, then the results seen by Hao *et. al.* appear to make sense.

To overcome the slower heat transfer rate of the continuous tubular reactor, the tube diameter must be decreased and/or the heat of the furnace must be set higher to increase the heat transfer gradient. Neither solution is desirable as using smaller tubing is not practical for eventual scale up operations and higher temperatures may exceed the limits of the materials, adding a safety concern.

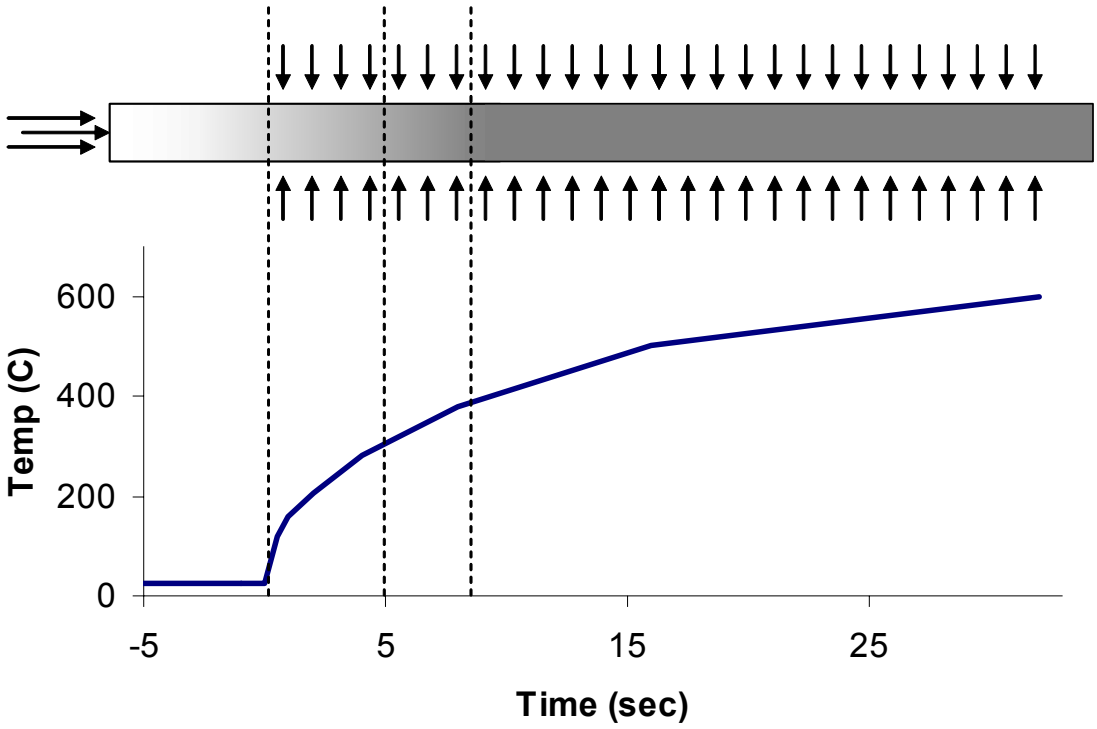

Figure 6.7 Temperature profile of substrate as it travels down the heated portion of the tubular reactor.

6.4.2 Continuous Reactor with Mixing Tee

In an effort to rapidly heat up the substrate to supercritical conditions, a mixing tee was implemented as shown in Figure 6.1. The organic feed entered the mixing tee at a relatively low temperature and mixed with the superheated supercritical water feed. The organic stream enters the mixing tee at a temperature range of 180-200ºC because the mixing tee was heated through conduction and via convective heat flow from the two adjacent furnaces.

The volume and corresponding time for mixing is difficult to assess due to entropies of mixing and phase change. However, it is reasonable to assume the heat up occurs much faster compared to the tubular reactor. The necessary heat was added to the water stream by conduction as it passed through the heater. That heat was then transferred to the cold stream by a combination of convection and mixing in a relatively small volume of less than 0.007 ml. Assuming the organic stream reaches supercritical conditions in the mixing tee (as indicated by the thermocouple readings), the residence time in the mixing tee would be approximately 0.12 seconds with a total flow rate of 3.4 ml/min. Under comparable conditions, a tubular reactor would need approximately 5 seconds for the temperature to rise from 250 to 380ºC, allowing for a longer residence time for the charring reactions to take place.

The mixing tee gives a possible explanation as to why the KOH catalyzed reactions ran so poorly. KOH will catalyze the hydrolysis of glucose at much lower temperatures, as discussed in Section 6.4.2. Due to the heat conducted through the tubing, the glucose enters the mixing tee already partially hydrolyzed and possibly inhibiting the gasification process.

The higher feed of 30% glucose may not work with the mixing tee for two potential reasons. Despite the rapid heating of the substrate, a temperature gradient still exists. If the char reaction is dependant upon the glucose reaction, the higher feed concentration will increase the char reaction rate. The higher glucose concentration will increase both the density and viscosity of the solution. Without any agitation, the viscous glucose solution and superheated water stream may not be readily miscible.

6.5 CONCLUSIONS

The factorial experiments show that higher temperatures contribute to higher gasification efficiencies. Given the endothermic nature of this process, this result is not surprising. The presence of homogeneous KOH catalyst negatively affected the efficiency. Increasing the residence time from 12 seconds to 40 seconds had no effect. This is good news in terms of process viability and shorter residence times should be explored. The continuous microreactor completely gasified 10% and 20% glucose solutions, but 30% solutions were not as efficient.

The continuous reactor used in these experiments shows the importance of heat transfer rates when the substrate is in sub-critical conditions. This heat transfer step would present a severe disadvantage to a batch process, especially one that is large in scale. The heat transfer effect also shows the limitations of some of the continuous reactors that are currently being studied. While the current design of this reactor is also susceptible to these limitations, it can process twice the feed concentration of other continuous reactors found in the literature.

The rapid nature of the gasification reactions makes it difficult to determine intermediates in the overall process. It appears there is a kinetic consideration of the sub-critical water chemistry that interferes with subsequent supercritical water chemistry. However, given a rapid heat transfer rate, the sub-critical water reactions can be overcome even with more complicated molecules. This observation may be critical when evaluating more complex molecules such as cellulose and lignins.

6.6 REFERENCES

1. Kirillin VA, Zubarev VN, *Teploenergetika*, 1955,19-23.

2. Arai Y, Sako T, Takebayashi. Supercritical Fluids: Molecular Interactions, Physical Properties, and New Applications. Berlin, Springer. 2002.

3. Lee IG, Kim MS, Ihm SK. Gasification of Glucose in Supercritical Water. *Ind. Eng. Chem. Res.* 2002, 41:1182-1188.

4. Hao, X. H.; Guo, L. J.; Mao, X.; Zhang, X. M.; Chen, X. J. Hydrogen Production from Glucose as a Model Compound of Biomass Gasified in Supercritical Water. *Int. J. Hydrogen Energy.* 2003, 28:55-64.

5. Box GEP, Hunter WG, Hunter JS. Statistics for Experimenters. New York: John Wiley & Sons, 1978.

6. Sinag, A.; Kruse, A.; Schwarzkopf, V.; Key Compounds of the Hydropyrolysis of Glucose in Supercritical Water in the Presence of K_2CO_3. *Ind. Eng. Chem. Res*. 2003, 42:3516.

7. Watanabe, M.; Inomata, H.; Osada, M.; Sato, T.; Adschiri, T.; Arai, K. Catalytic effects of NaOH and ZrO_2 for partial oxidative gasification of n-hexadecane and lignin in supercritical water. *Fuel* 2003, 82:545.

8. Williams PT and Onwudili J. Composition of Products from the Supercritical Water Gasification of Glucose: A Model Biomass Compound. *Ind. Eng. Chem. Res.* 2005**,** 44:8739-8749.

9. Matsumura Y, Minowa T, Potic B, Kersten SRA, Prins W, van Swaaij WPM, van de Beld B, Elliott DC, Neuenschwander GG, Kruse A, Antal MJ. Biomass Gasification in Near- and Supercritical Water: Status and Prospects. *Biomass Bioenergy* 2005, 29:269..

10. Xu, X.; Matsumura, Y.; Stenberg, J.; Antal, M. J. Carbon-Catalyzed Gasification of Organic Feedstocks in Supercritical Water. *Ind. Eng. Chem. Res*. 1996, *35*, 2522.

11. Shafizadeh, F. Introduction to Pyrolysis of Biomass. *J. Anal. Appl. Pyrol.* 1982, 3:283.

12. Onwudili JA, Williams PT. Flameless Incineration of Pyrene Under Sub-critical and Supercritical Water Conditions. *Fuel*. 2006, 85:75-83.

7 CONCLUSIONS AND FUTURE WORK

7.1 PHOTOSYNTHETIC H_2 PRODUCTION

Using a statistical design of experiments was an effective way of screening out process variables that were significant to the production of H_2 gas in *Chlamydomonas reinhardtii*. When followed up by more in-depth investigations, important parameters were discovered, specifically concerning the reactor shape and light intensity, which will be important in future scale up operations. The binding experiments also showed how effective fumed silica particles can be used as a support medium as there was no detrimental effect on the production output. Silica support has the added advantages of eliminating an expensive processing step, being an inexpensive and readily available material, and easily incorporating into any future reactor design.

Manipulating the process variables for photosynthetic hydrogen production of *Chlamydomonas reinhardtii* was not enough to significantly increase the hydrogen output. Binding the algal cells did not increase photosynthetic efficiency either. The limiting factor appears to be the oxygen sensitivity of the algal cells, specifically the hydrogenase enzyme. Eliminating sulfates is an effective method of switching the algal cells to H_2 production mode but effectively decreases photosynthetic activity, choking off H_2 yields.

Future work must focus on making *C. reinhardtii* more oxygen tolerant, even viable, in an oxygen environment. If protons can undergo reduction with an oxygen

tolerant hydrogenase enzyme or some other methods that can work in conjunction with the photosystems, then some of the methods learned in this study may be incorporated to produce a viable hydrogen production system.

7.2 SUPERCRITICAL WATER GASIFICATION OF GLUCOSE

A new continuous supercritical water gasification reactor was built and used to study the thermochemical conversion of glucose. The new reactor design demonstrated the limitation of batch reactors, and some of the current continuous reactors, of not having the ability to heat up the feed at a sufficient rate. The higher heating rate allowed the new reactor to gasify glucose at twice the concentrations reported in the current literature. The new reactor system also showed how important heating rate is to the mechanism of the glucose gasification.

The conversion of glucose is only the first step in understanding how biomass can be used as a feedstock for hydrogen production. More complicated oligomers and polymers must next be studied. Ultimately, a multi-step approach may be needed to pyrolyze the biomass polymers (potentially with partial oxidation), followed by a rapid gasification to break down the monomeric components as explored in this work.

VITA

John Hahn was born in Seoul, Korea and moved to the United States at an early age. He grew up in New England and attended college at Clark University in Worcester, Massachusetts. After college, John Hahn moved to Columbia, Missouri where he met his wife Jessica.